Beam-energy and collision-system size dependence of the anisotropic flow measurements

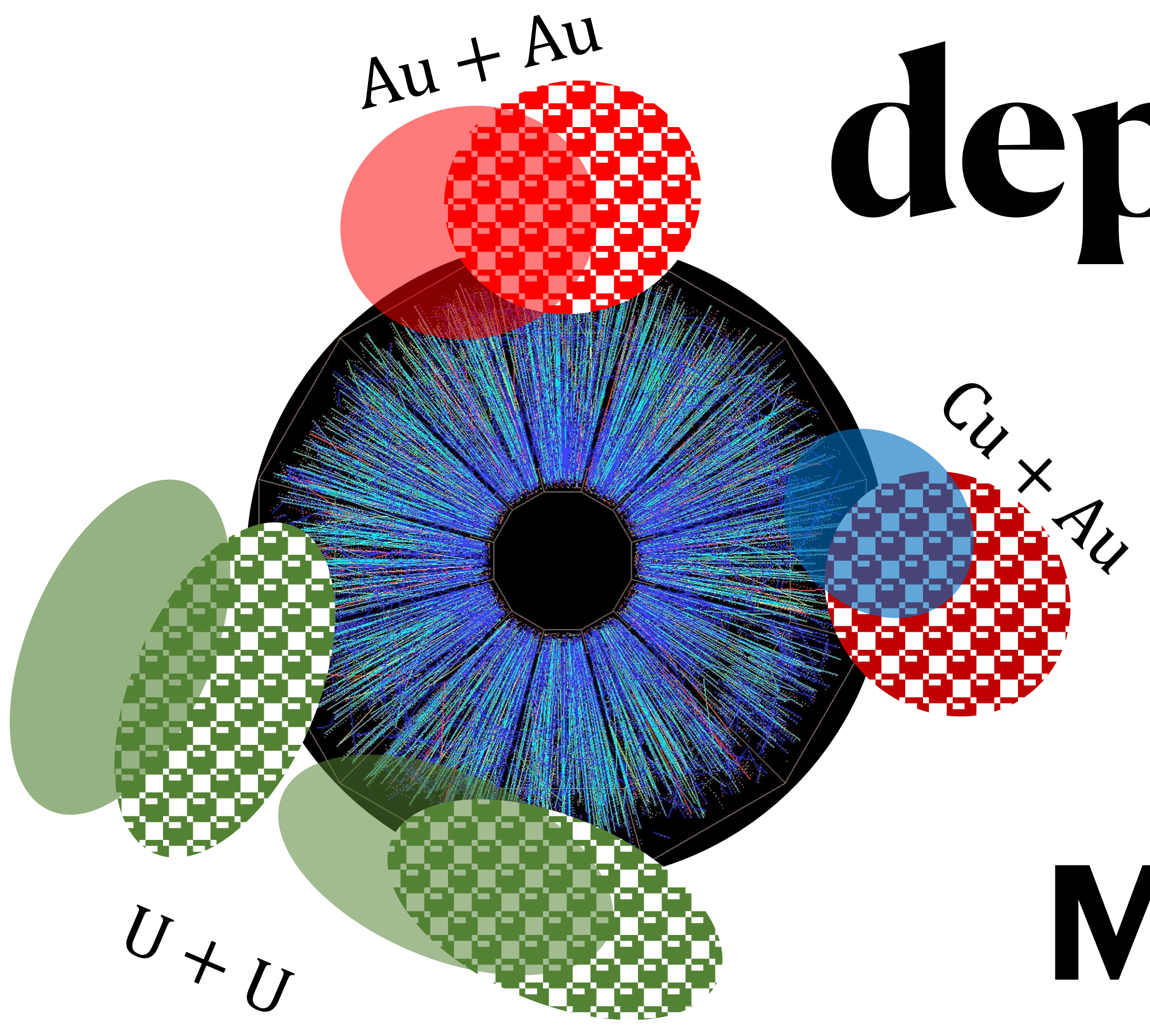

Maria Stefaniak for **STAR Collaboration**

STAR

POLITECHNIKA WARSZAWSKA
WARSAW UNIVERSITY OF TECHNOLOGY

Faculty of Physics
WARSAW UNIVERSITY OF TECHNOLOGY

Subatech

Institut Mines-Télécom

Anisotropic flow

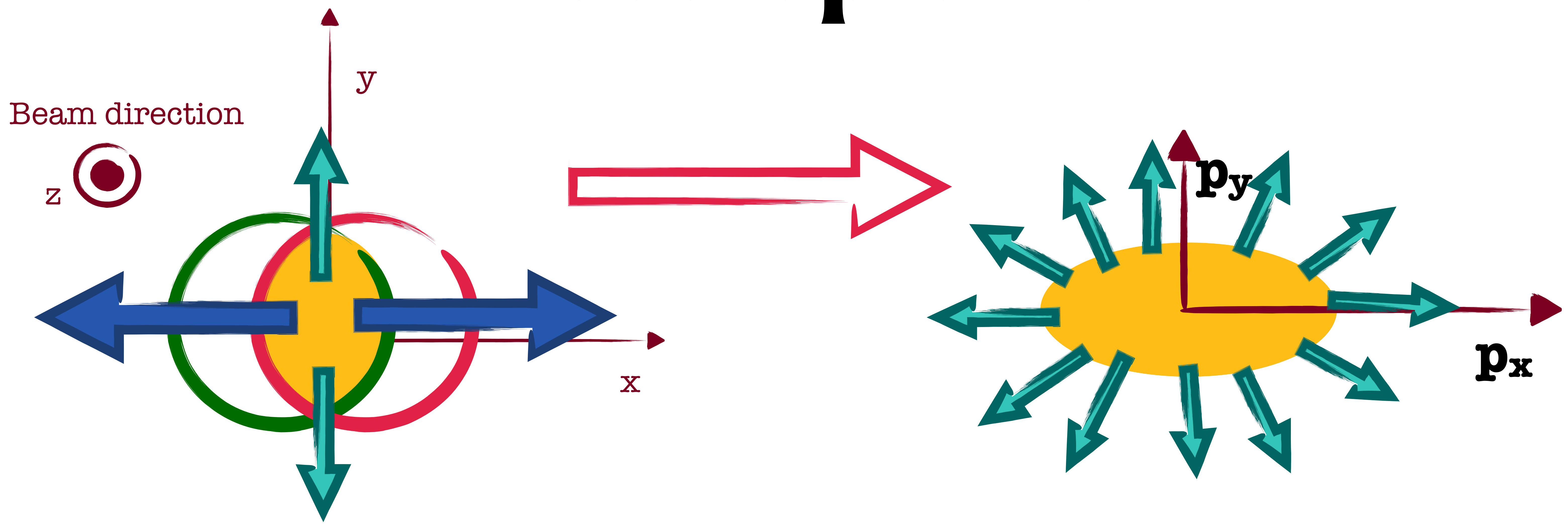

Anisotropy in initial geometry ⇒ Final-state momentum anisotropy

Anisotropic flow

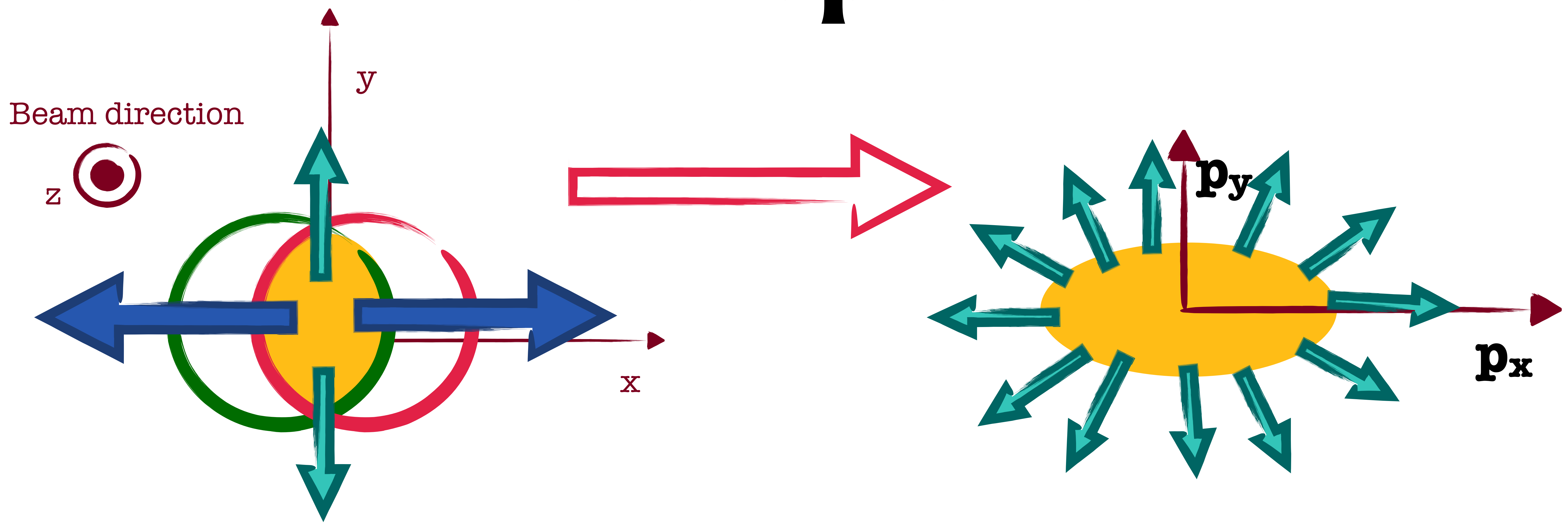

Anisotropy in initial geometry → **Final-state momentum anisotropy**

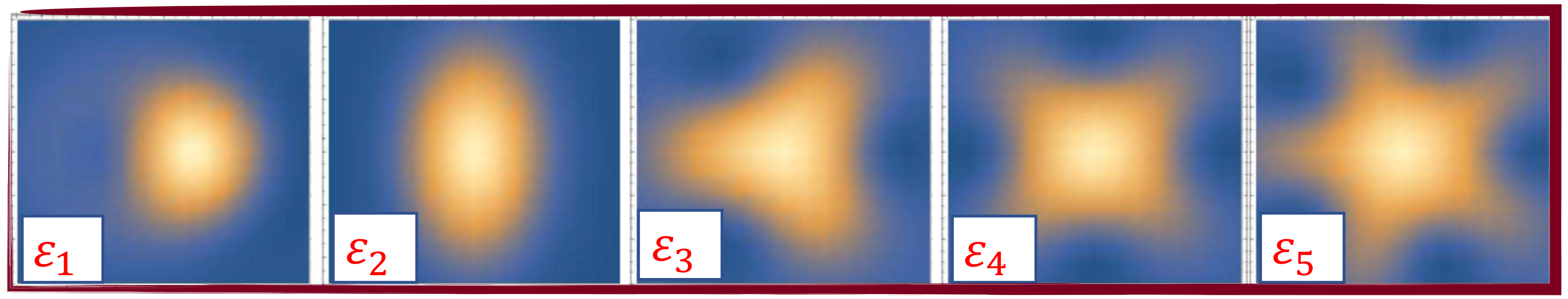

Anisotropic flow measurements are sensitive to:

- Initial-state spatial anisotropy
- Flow fluctuations and correlations
- Transport properties (i.e., $\frac{\eta}{s}, \frac{\zeta}{s}, \frac{\hat{q}}{T^3}$,...)

Anisotropic flow

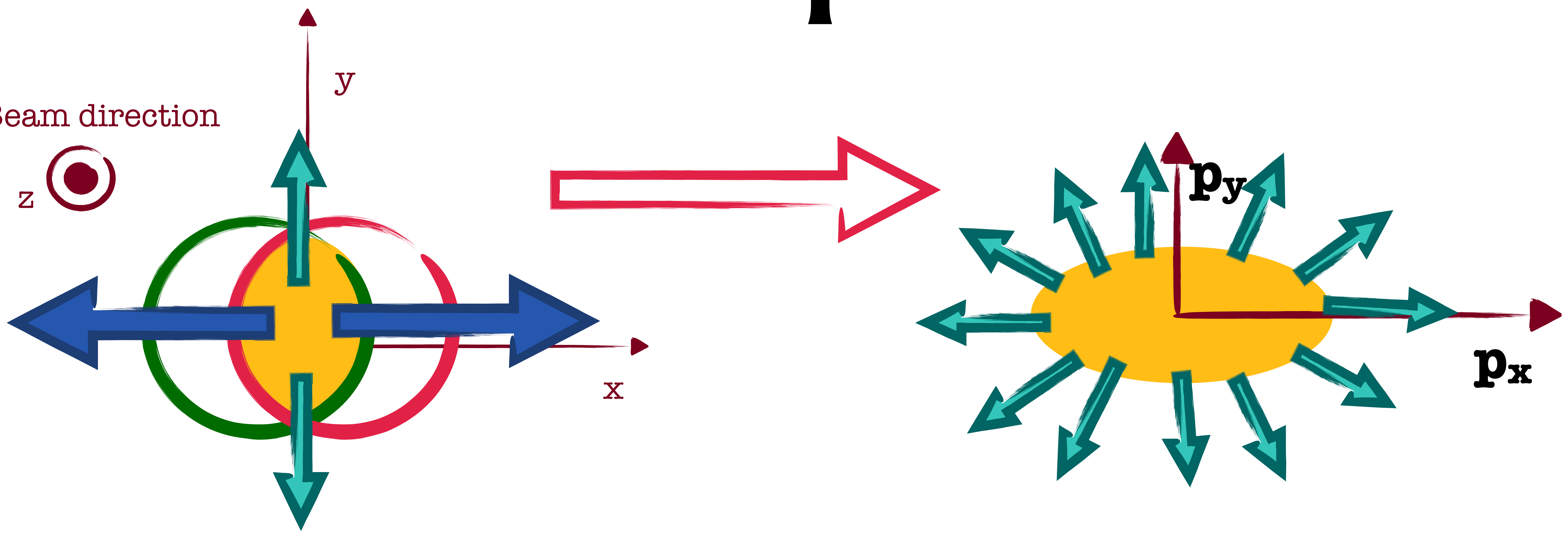

Anisotropy in initial geometry ⇒ **Final-state momentum anisotropy**

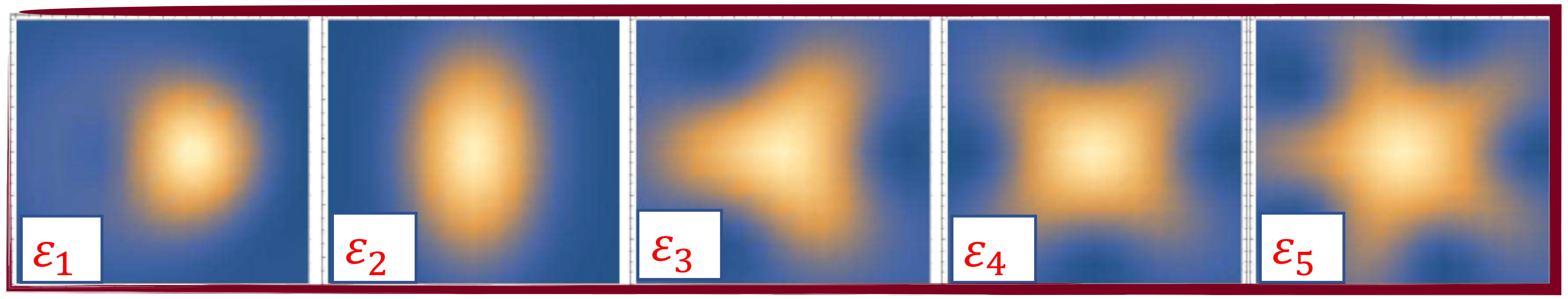

Anisotropic flow measurements are sensitive to:

- Initial-state spatial anisotropy
- Flow fluctuations and correlations
- Transport properties (i.e., $\frac{\eta}{s}, \frac{\zeta}{s}, \frac{\hat{q}}{T^3}$,...)

What are the respective roles of ε_n and its fluctuations, flow correlations and transport properties on the v_n?

Anisotropic flow

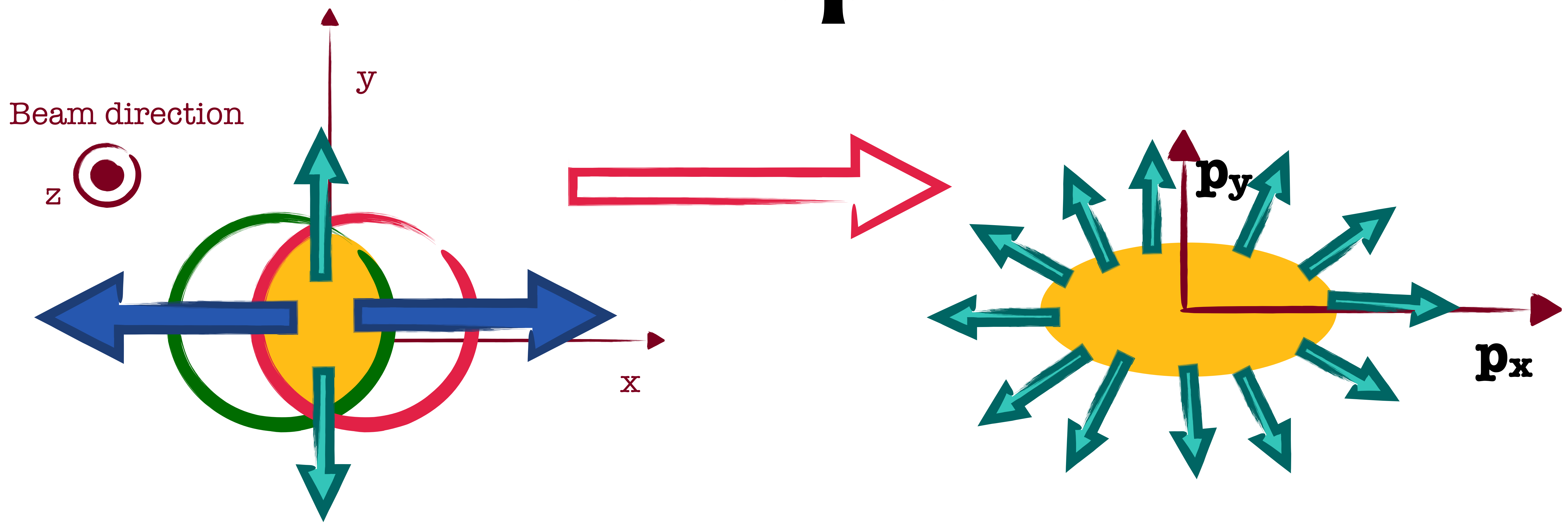

Anisotropy in initial geometry ⇒ **Final-state momentum anisotropy**

Outline:
- PID flow harmonics
- Flow decorrelation
- High p_T flow harmonics

The Solenoid Tracker At RHIC Experiment

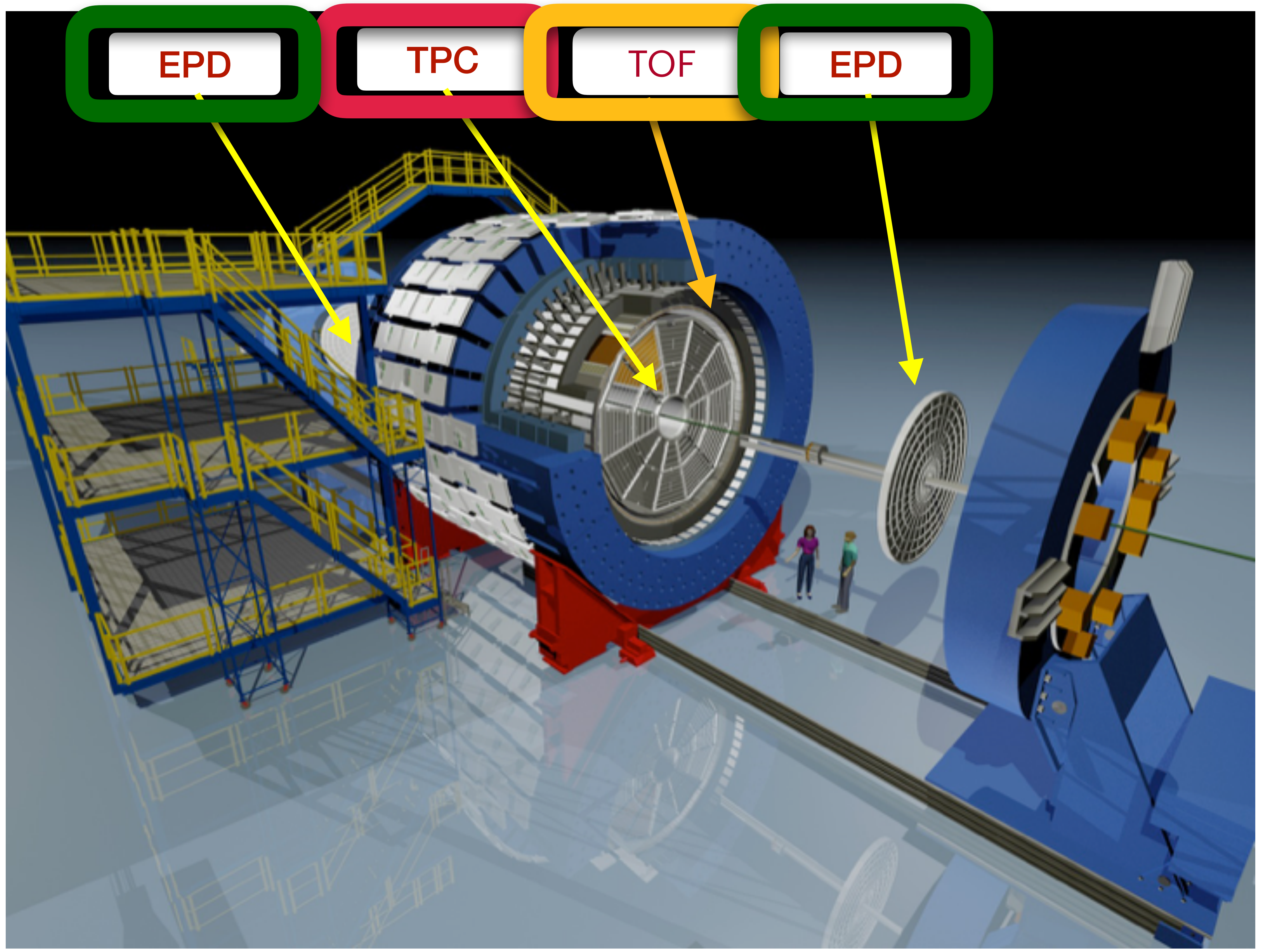

Time Projection Chamber

Tracking charged particles with:

- Full azimuthal coverage
- $|\eta|<1$ coverage
- Particle Identification

Time-Of-Flight

- Particle identification (high momentum)

Event Plane Detector

- Acceptance : $2.1 < |\eta| < 5.1$.

Identified hadrons flow harmonics:

2-particle correlations (2PC)

$$c_n\{2\} = \langle\langle 2 \rangle\rangle_{a|b} = \langle\langle e^{in(\phi_1^a - \phi_2^b)} \rangle\rangle = \frac{\langle\langle Q_{n,a} Q_{n,b}^* \rangle\rangle}{\langle\langle M_a M_b \rangle\rangle}$$

- The non-flow contribution is reduced with $\Delta\eta$ gap

Integrated & **p_T (PID) - differential flow harmonics**

$$v_n\{2\} = \sqrt{c_n\{2\}}$$

$$v_n(p_T) = v_n^2(p_T, p_T^{ref}) / \sqrt{v_n^2(p_T^{ref}, p_T^{ref})}$$

STAR

Identified hadrons flow harmonics:

2-particle correlations (2PC)

$$c_n\{2\} = \langle\langle 2 \rangle\rangle_{a|b} = \langle\langle e^{in(\phi_1^a - \phi_2^b)} \rangle\rangle = \frac{\langle\langle Q_{n,a} Q^*_{n,b} \rangle\rangle}{\langle\langle M_a M_b \rangle\rangle}$$

- The non-flow contribution is reduced with $\Delta\eta$ gap

Integrated & **p_T (PID) - differential flow harmonics**

$$v_n\{2\} = \sqrt{c_n\{2\}} \qquad v_n(p_T) = v_n^2(p_T, p_T^{ref}) / \sqrt{v_n^2(p_T^{ref}, p_T^{ref})}$$

Integrated flow harmonics

	Hydro−1	Hydro−2
η/s	0.05	0.12
Initial conditions	TRENTO	IP-Glasma
Contributions	Hydro + Direct decays	Hydro + Hadronic cascade

(1) P. Alba, et al. PRC 98 , 034909 (2018)

(2) B.Schenke, et al. PRC 99, 044908 (2019)

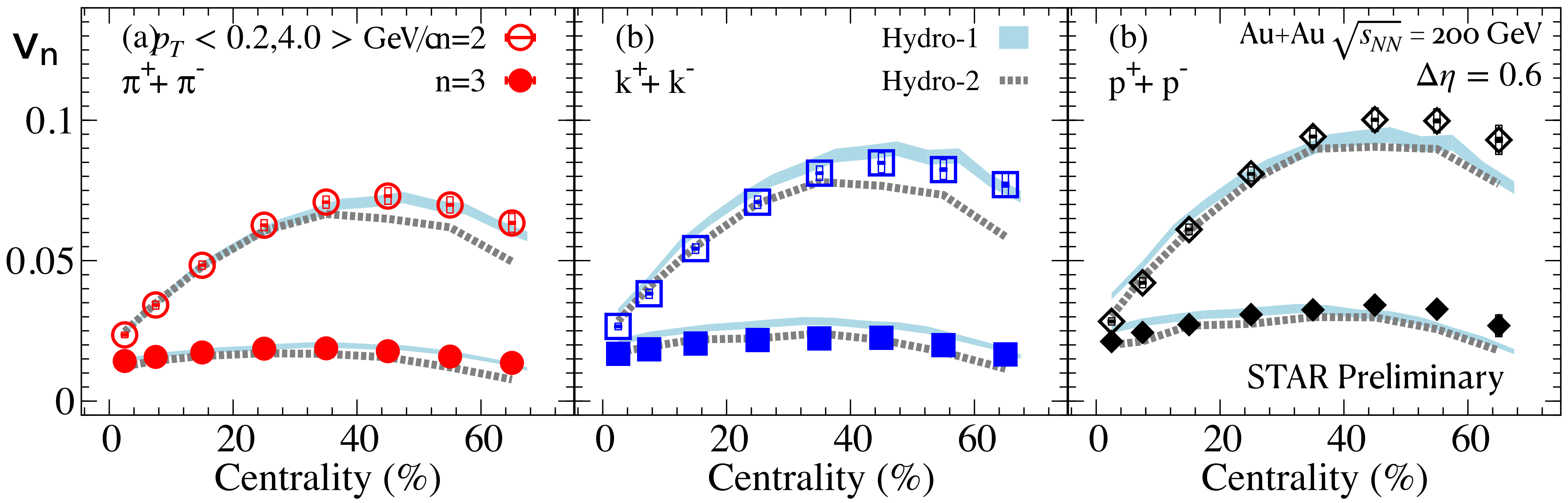

- Both hydro simulations reproduce qualitatively v_n collisions for Au+Au at $\sqrt{s_{NN}} = 200$ GeV

Identified hadrons flow harmonics:

2-particle correlations (2PC)

$$c_n\{2\} = \langle\langle 2 \rangle\rangle_{a|b} = \langle\langle e^{in(\phi_1^a - \phi_2^b)} \rangle\rangle = \frac{\langle\langle Q_{n,a} Q^*_{n,b} \rangle\rangle}{\langle\langle M_a M_b \rangle\rangle}$$

- The non-flow contribution is reduced with $\Delta\eta$ gap

Integrated & **p_T (PID) - differential flow harmonics**

$v_n\{2\} = \sqrt{c_n\{2\}}$

$v_n(p_T) = v_n^2(p_T, p_T^{ref}) / \sqrt{v_n^2(p_T^{ref}, p_T^{ref})}$

- Both hydro simulations reproduce qualitatively v_n collisions for Au+Au at $\sqrt{s_{NN}} = 200$ GeV
- Eccentricity does not differ relevantly between collision energies ➜ differences (~5%) caused by transitions in transport coefficients

Integrated flow harmonics

	Hydro−1	Hydro−2
η/s	0.05	0.12
Initial conditions	TRENTO	IP-Glasma
Contributions	Hydro + Direct decays	Hydro + Hadronic cascade

(1) P. Alba, et al. PRC 98 , 034909 (2018)
(2) B.Schenke, et al. PRC 99, 044908 (2019)

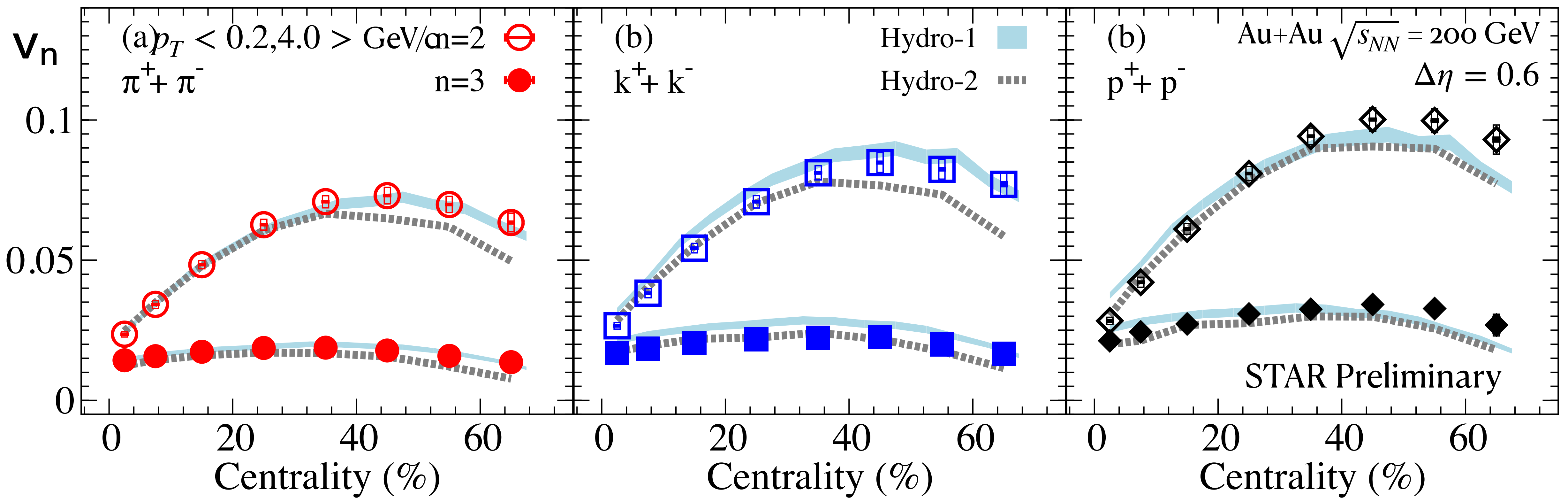

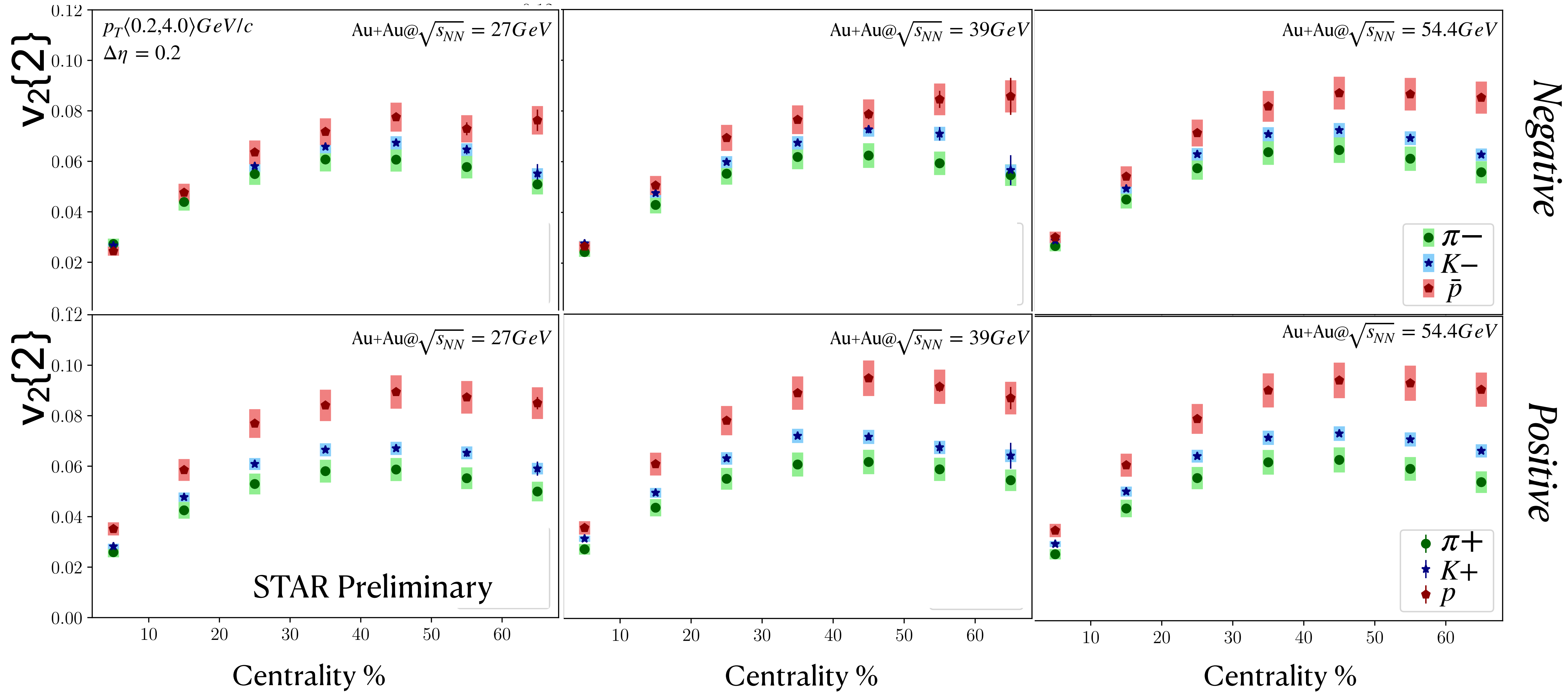

Identified hadrons flow harmonics:

2-particle correlations (2PC)

$$c_n\{2\} = \langle\langle 2 \rangle\rangle_{a|b} = \langle\langle e^{in(\phi_1^a - \phi_2^b)} \rangle\rangle = \frac{\langle\langle Q_{n,a} Q^*_{n,b} \rangle\rangle}{\langle\langle M_a M_b \rangle\rangle}$$

- The non-flow contribution is reduced with $\Delta\eta$ gap

Integrated & **p_T (PID) - differential flow harmonics**

$$v_n\{2\} = \sqrt{c_n\{2\}} \qquad v_n(p_T) = v_n^2(p_T, p_T^{ref}) / \sqrt{v_n^2(p_T^{ref}, p_T^{ref})}$$

- Both hydro simulations reproduce qualitatively v_n collisions for Au+Au at $\sqrt{s_{NN}} = 200$ GeV
- Eccentricity does not differ relevantly between collision energies ➜ differences (~5%) caused by transitions in transport coefficients

Integrated flow harmonics

	Hydro−1	Hydro−2
η/s	0.05	0.12
Initial conditions	TRENTO	IP-Glasma
Contributions	Hydro + Direct decays	Hydro + Hadronic cascade

(1) P. Alba, et al. PRC 98 , 034909 (2018)
(2) B.Schenke, et al. PRC 99, 044908 (2019)

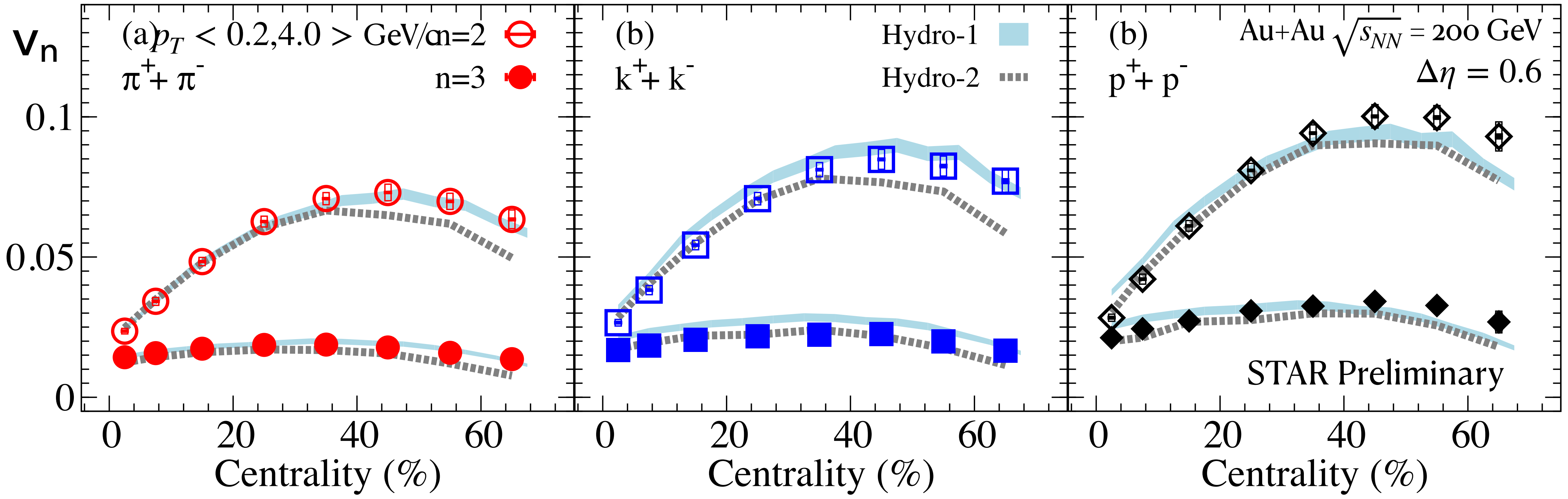

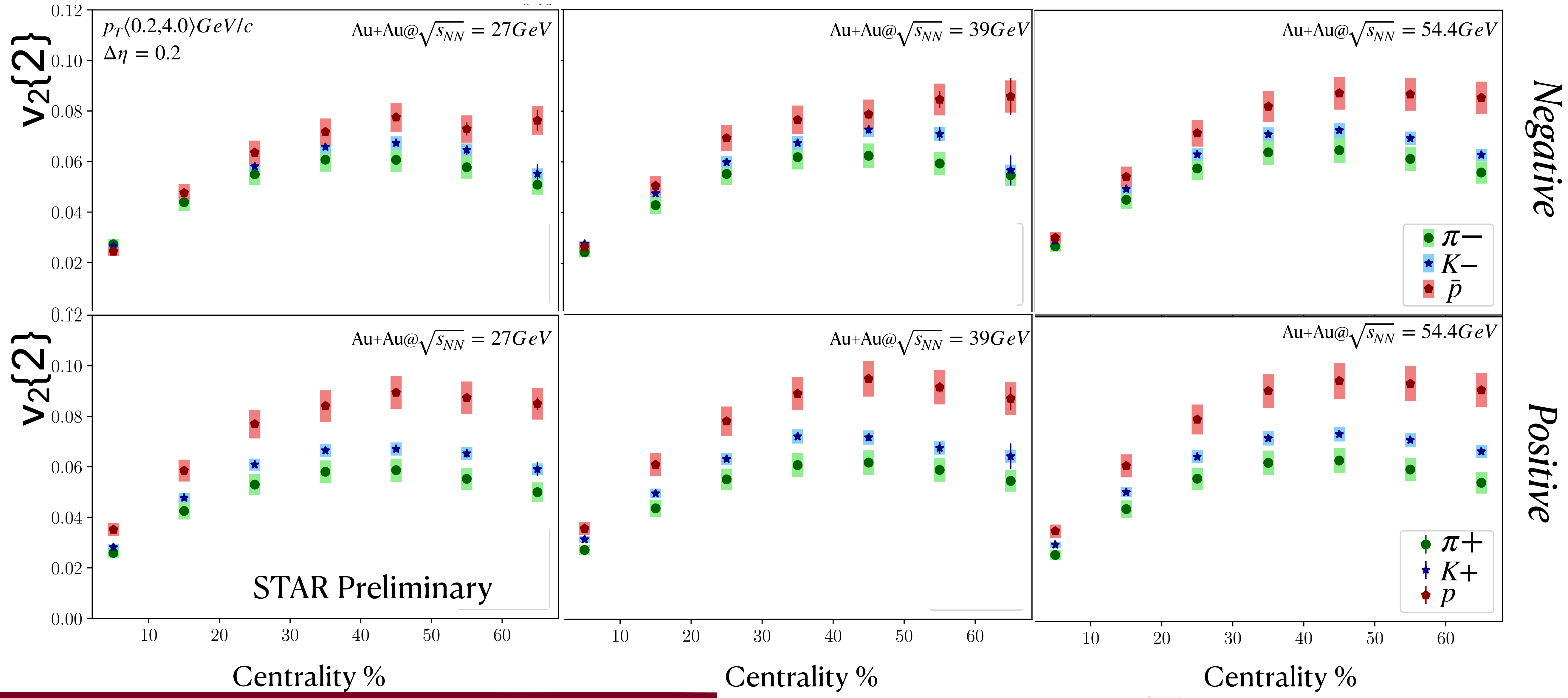

Excellent constrain for the hydrodynamical models

STAR

Identified hadrons flow harmonics:

$\sqrt{s_{NN}} = 200$ GeV

pT (PID) - differential flow harmonics

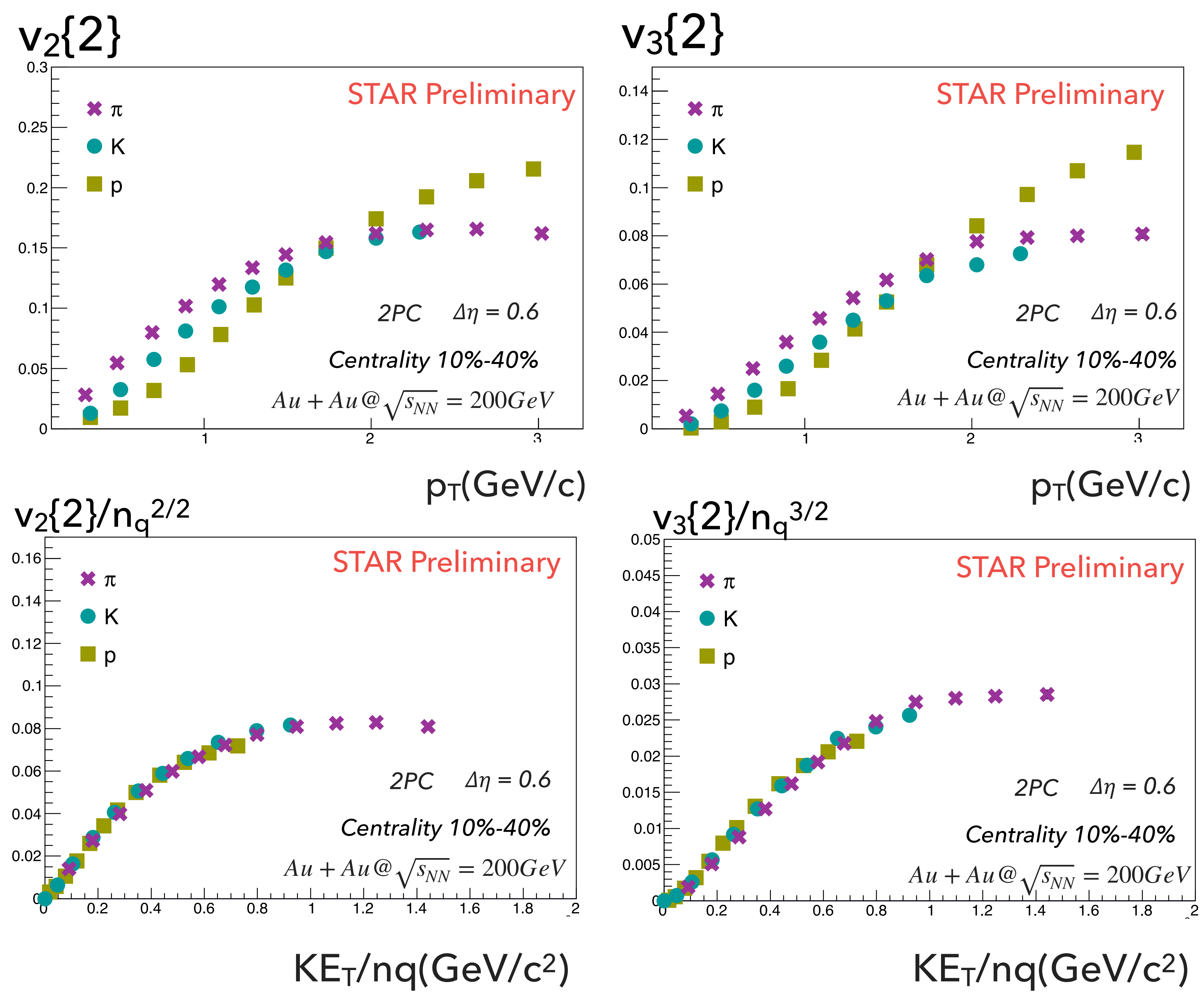

- Visible mass ordering for both harmonics and energies

Identified hadrons flow harmonics:

$\sqrt{s_{NN}} = 200$ GeV

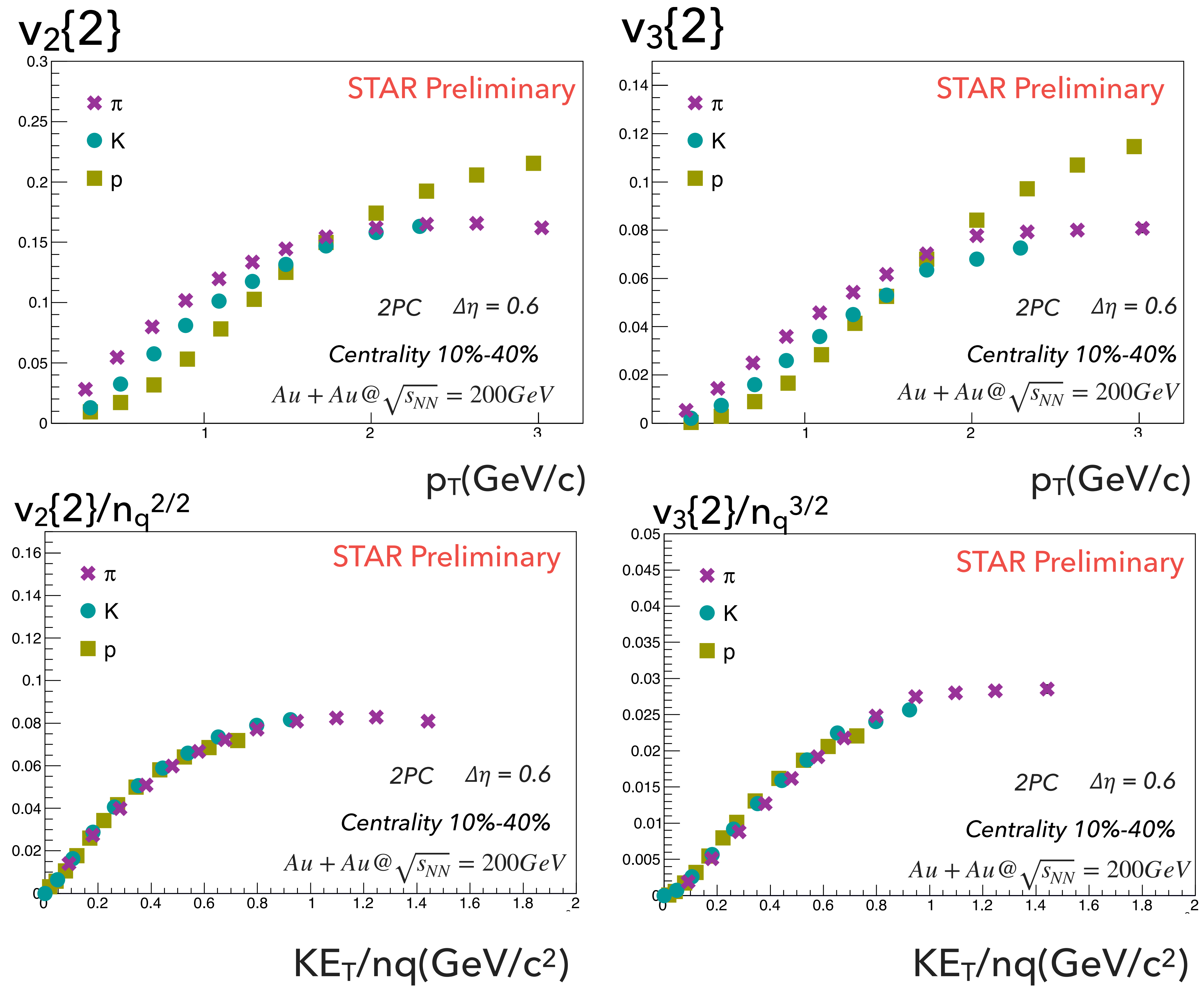

p_T (PID) - differential flow harmonics

$\sqrt{s_{NN}} = 39$ GeV

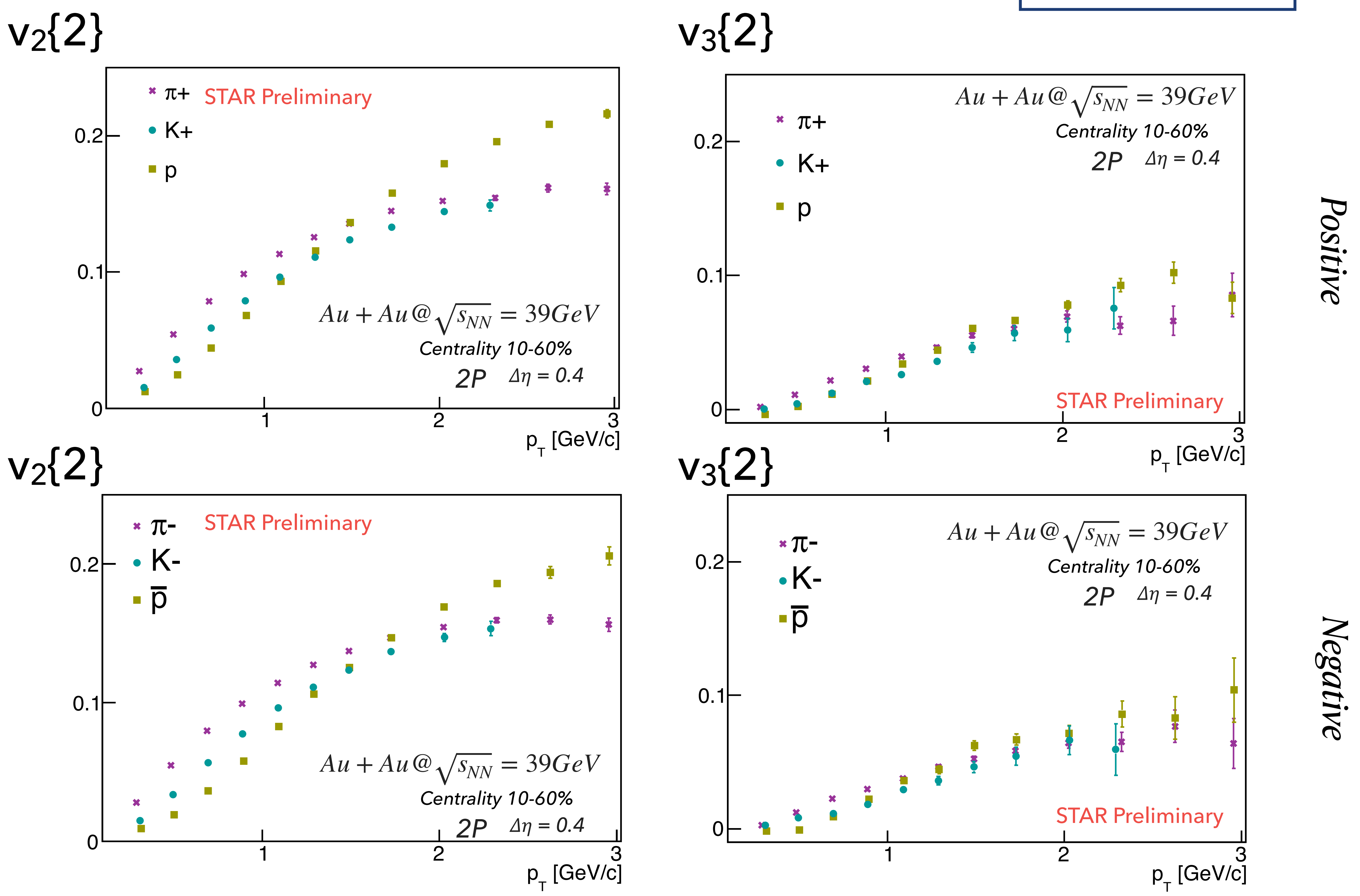

- Visible mass ordering for both harmonics and energies

Identified hadrons flow harmonics:

p_T (PID) - differential flow harmonics

$\sqrt{s_{NN}} = 200$ GeV

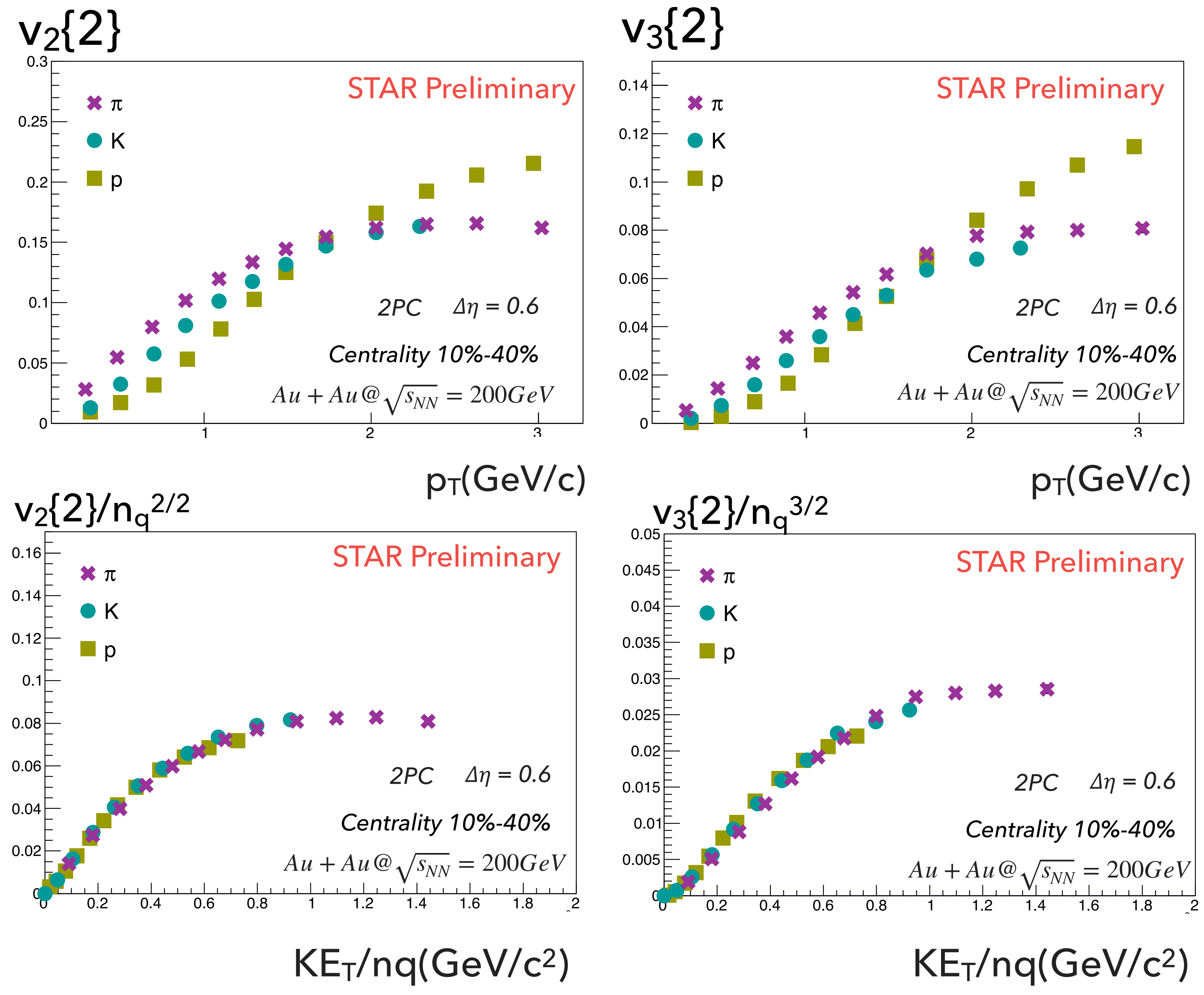

$\sqrt{s_{NN}} = 39$ GeV

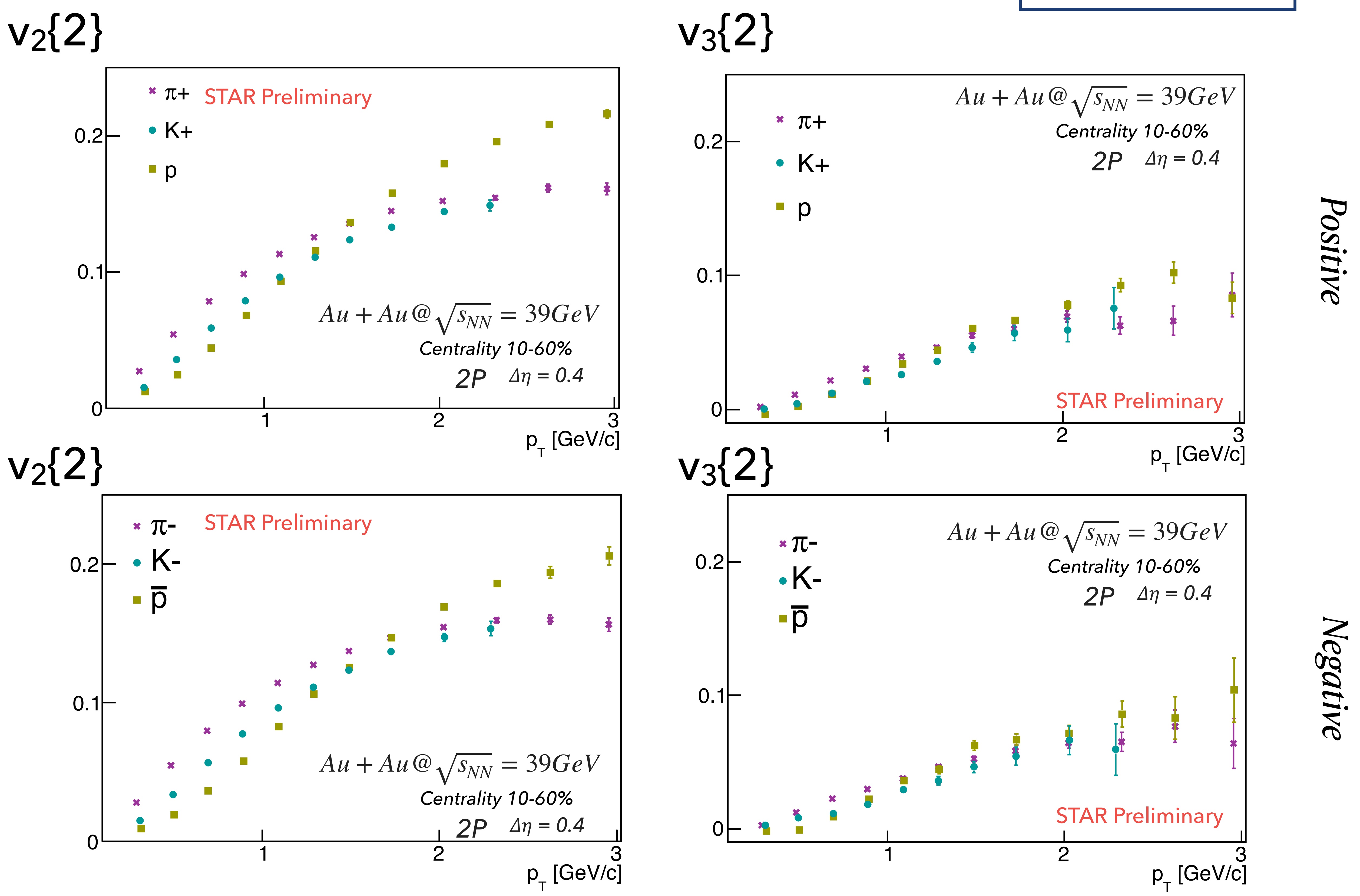

- Visible mass ordering for both harmonics and energies

Odd ϵ_n coefficients vanish because of symmetry $\phi \rightarrow (-\phi)$ or $\phi \rightarrow (\phi + \pi)$

Triangular flow - more sensitive to **fluctuations** than elliptic flow

Identified hadrons flow harmonics:

p_T (PID) - differential flow harmonics

$\sqrt{s_{NN}} = 200$ GeV

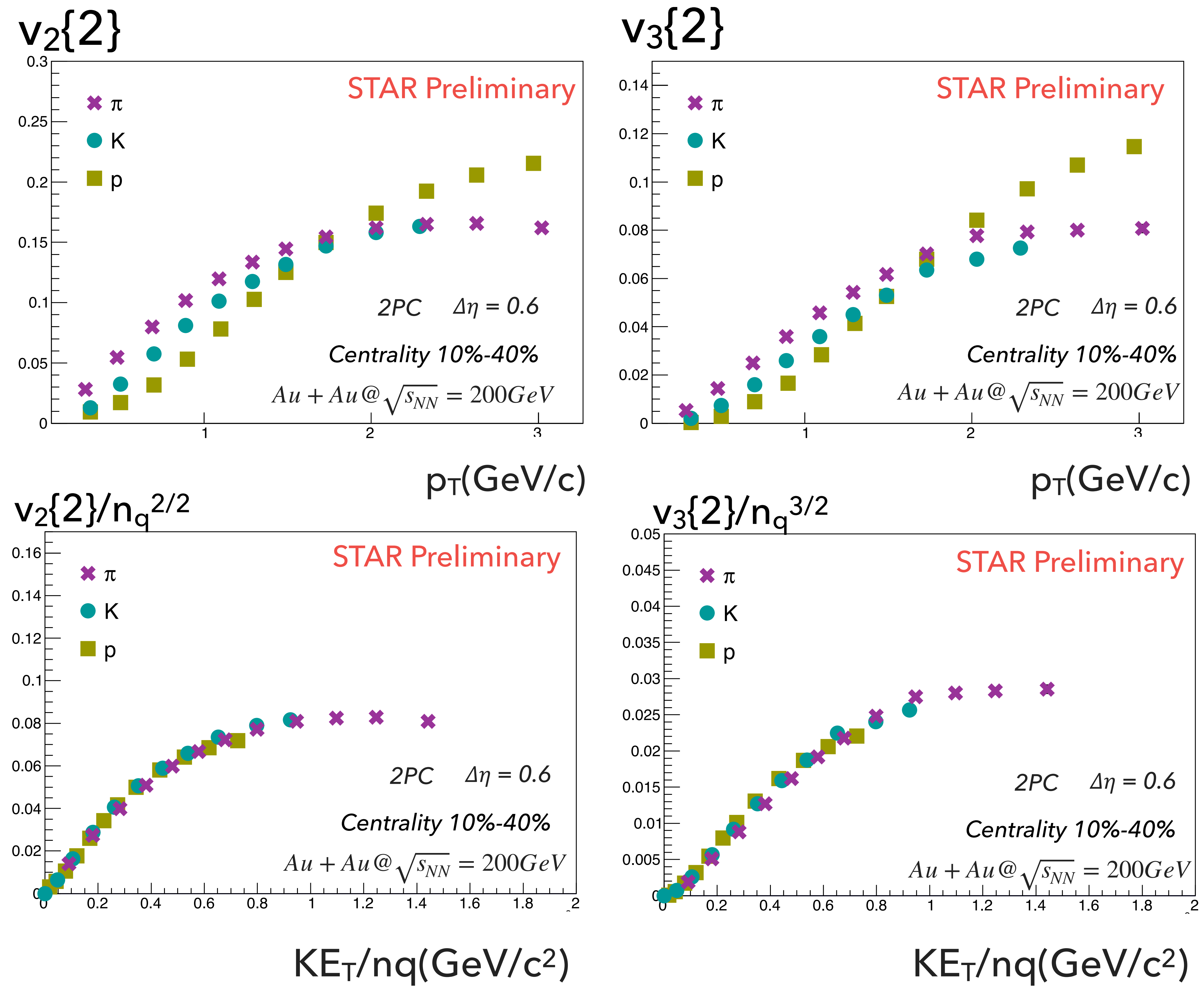

$\sqrt{s_{NN}} = 39$ GeV

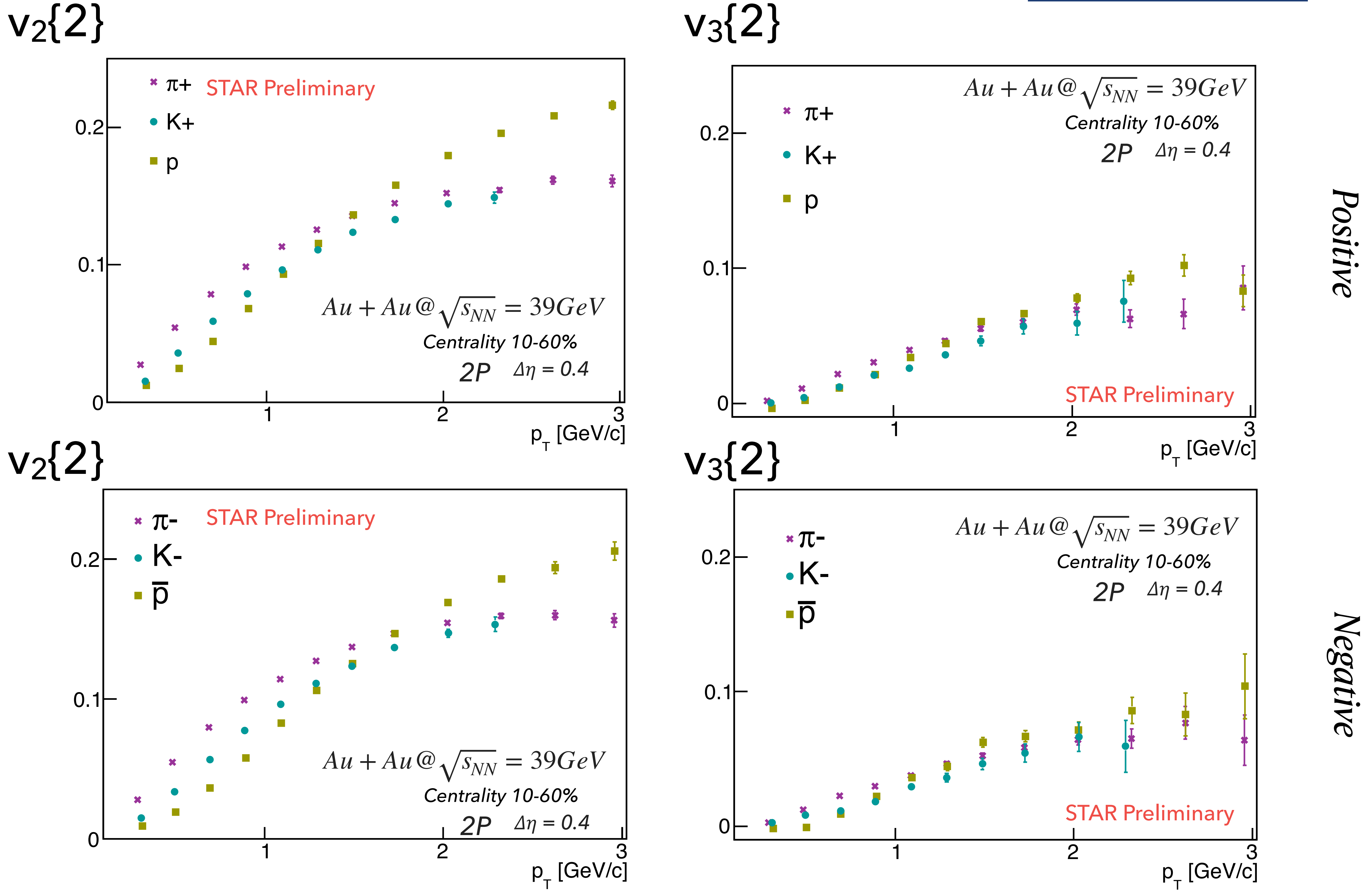

- Visible mass ordering for both harmonics and energies

Odd ϵ_n coefficients vanish because of symmetry
$\phi \rightarrow (-\phi)$ **or** $\phi \rightarrow (\phi + \pi)$

Triangular flow - more sensitive to **fluctuations** than elliptic flow

Significant reference for the theoretical studies of initial fluctuation and QGP

(Anti)particle v_n difference in $\sqrt{s_{NN}}$

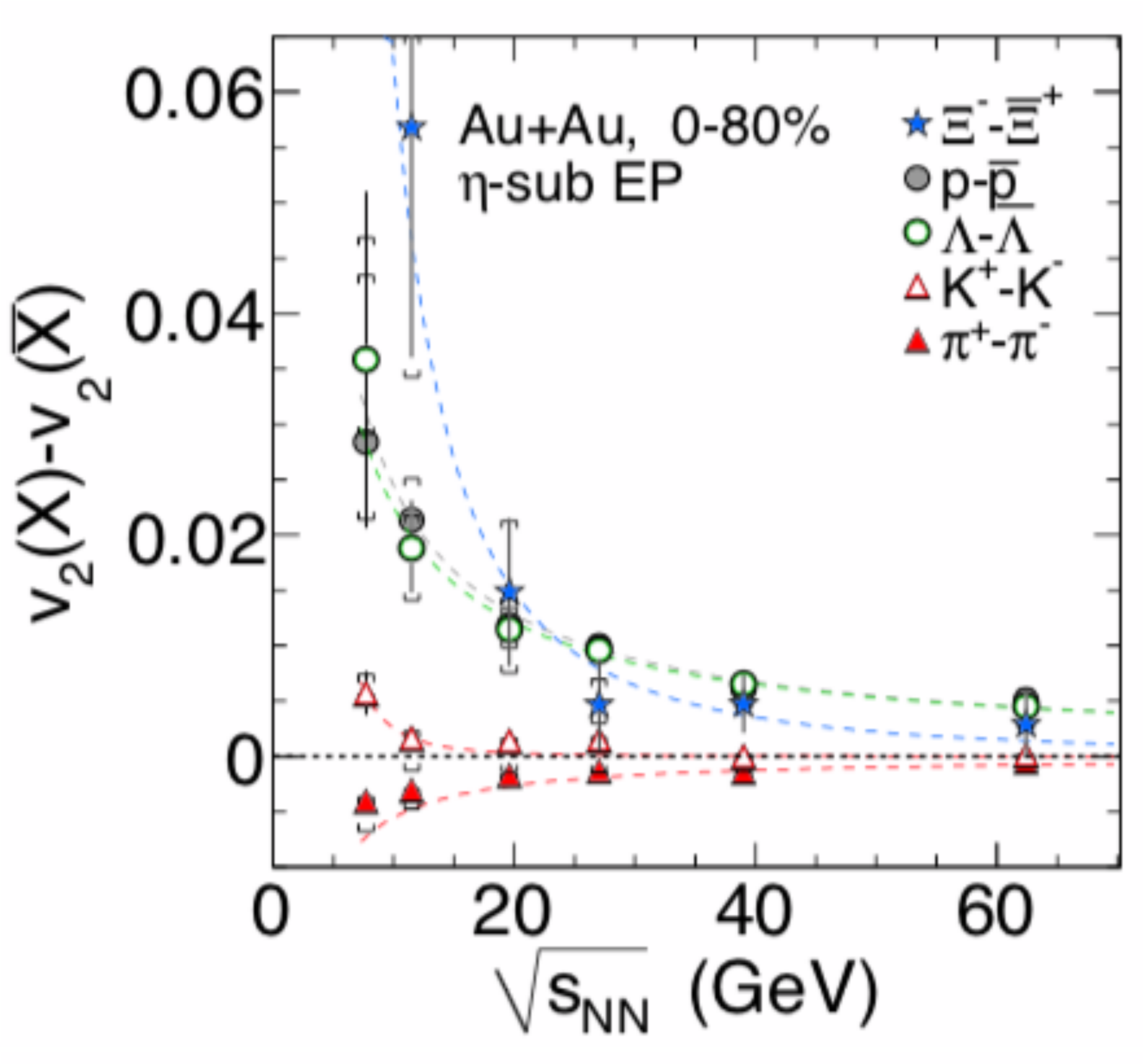

- Difference of protons - antiprotons elliptic flow increases with decreasing collision energy

STAR Collaboration: Phys. Rev. C 88 (2013) 14902

Identified hadrons flow harmonics: Au+Au @ BES

(Anti)particle v_n difference in $\sqrt{s_{NN}}$

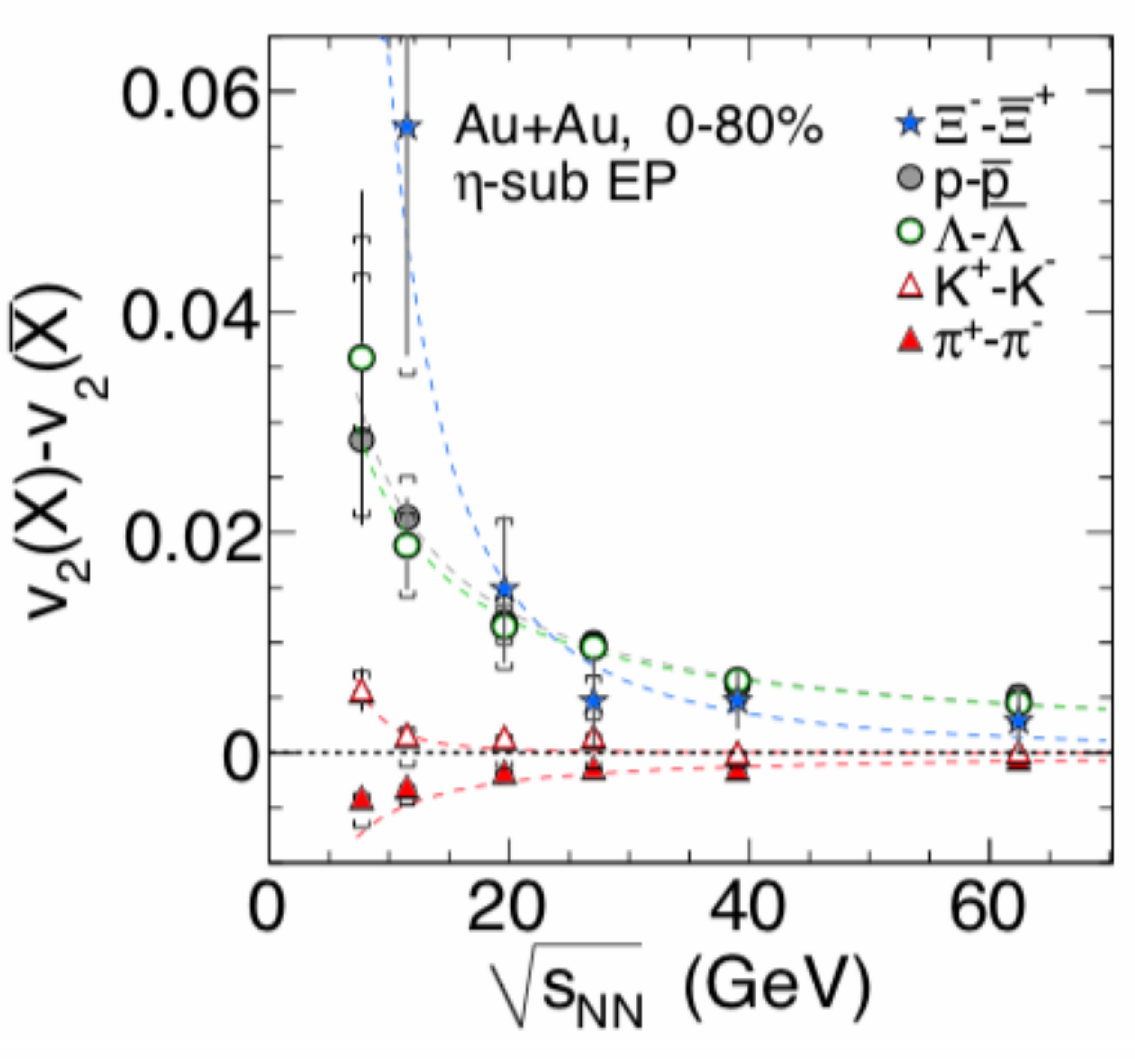

- Difference of protons - antiprotons elliptic flow increases with decreasing collision energy

STAR Collaboration: Phys. Rev. C 88 (2013) 14902

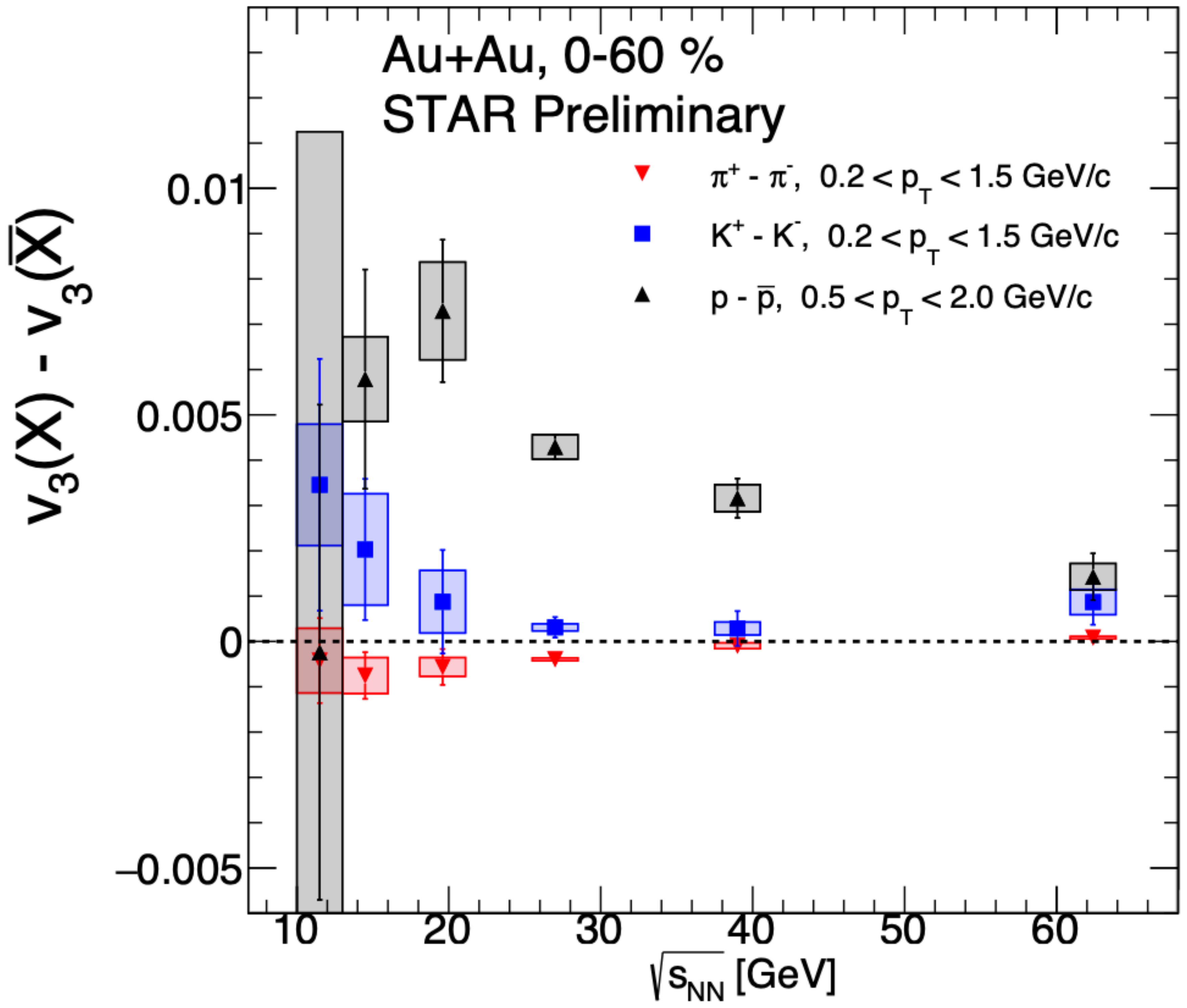

- Similar trends for differences in triangular flow

STAR Collaboration: J. Phys.: Conf. Ser. 1690 012128

Longitudinal flow correlations

For more information please see **Maowu Nie** poster:
https://indico.cern.ch/event/854124/contributions/4135474/

◆ Fluctuation of sources in two nuclei

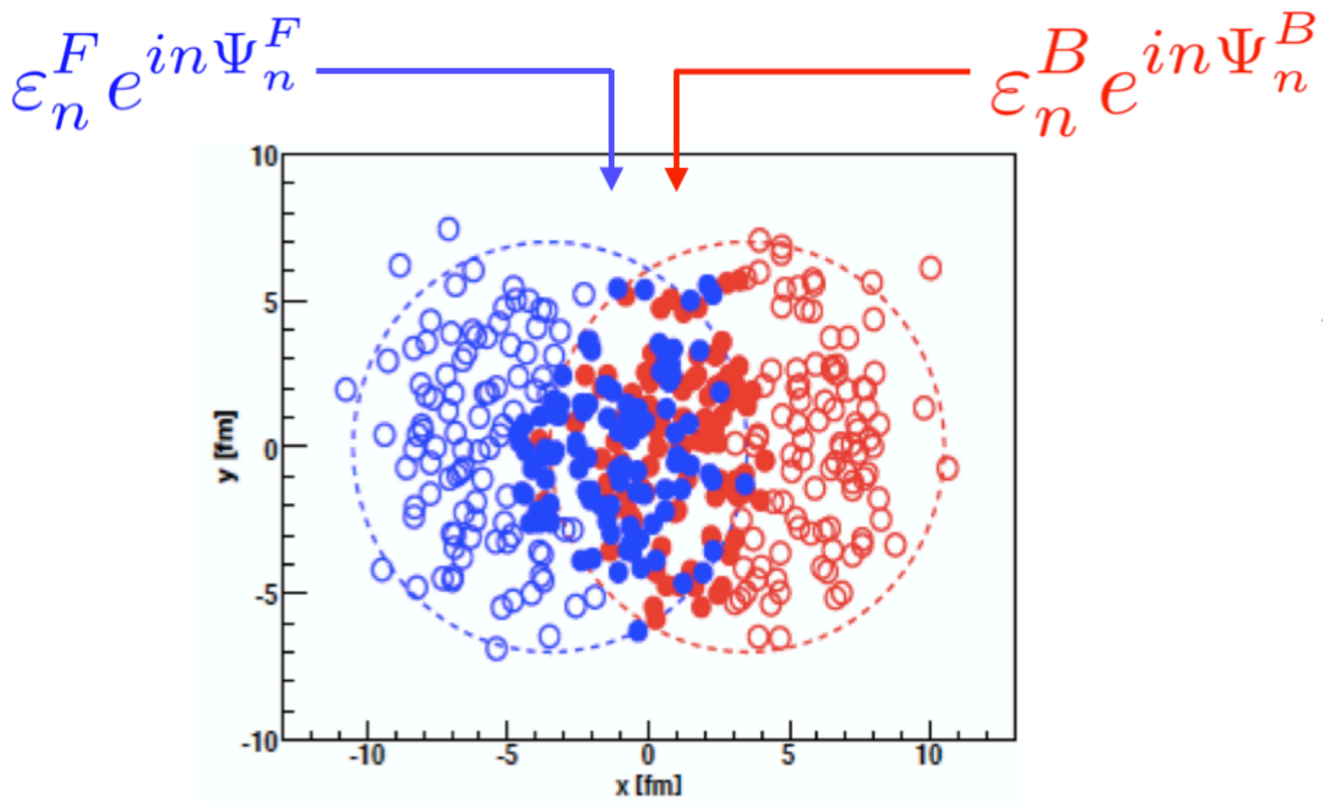

◆ Factorization ratio, r_n, is constructed as a measure of the flow decorrelation

CMS Collaboration: Phys. Rev. C 92 (2015) 034911

$$r_n(\eta) = \frac{\langle V_n(-\eta)V_n^*(\eta_{\mathrm{ref}})\rangle}{\langle V_n(\eta)V_n^*(\eta_{\mathrm{ref}})\rangle} = \frac{\langle v_n(-\eta)v_n(\eta_{\mathrm{ref}})\cos n(\Psi_n(-\eta)-\Psi_n(\eta_{\mathrm{ref}}))\rangle}{\langle v_n(\eta)v_n(\eta_{\mathrm{ref}})\cos n(\Psi_n(\eta)-\Psi_n(\eta_{\mathrm{ref}}))\rangle}$$

◆ Evolution of the QGP in (3+1)D

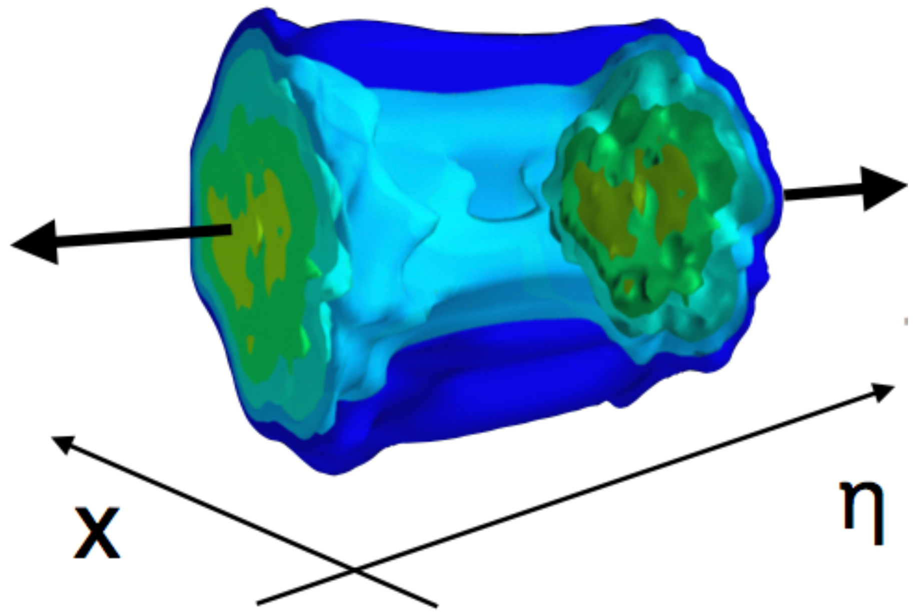

◆ r_n measures relative fluctuation between $v_n(-\eta)$ and $v_n(\eta)$

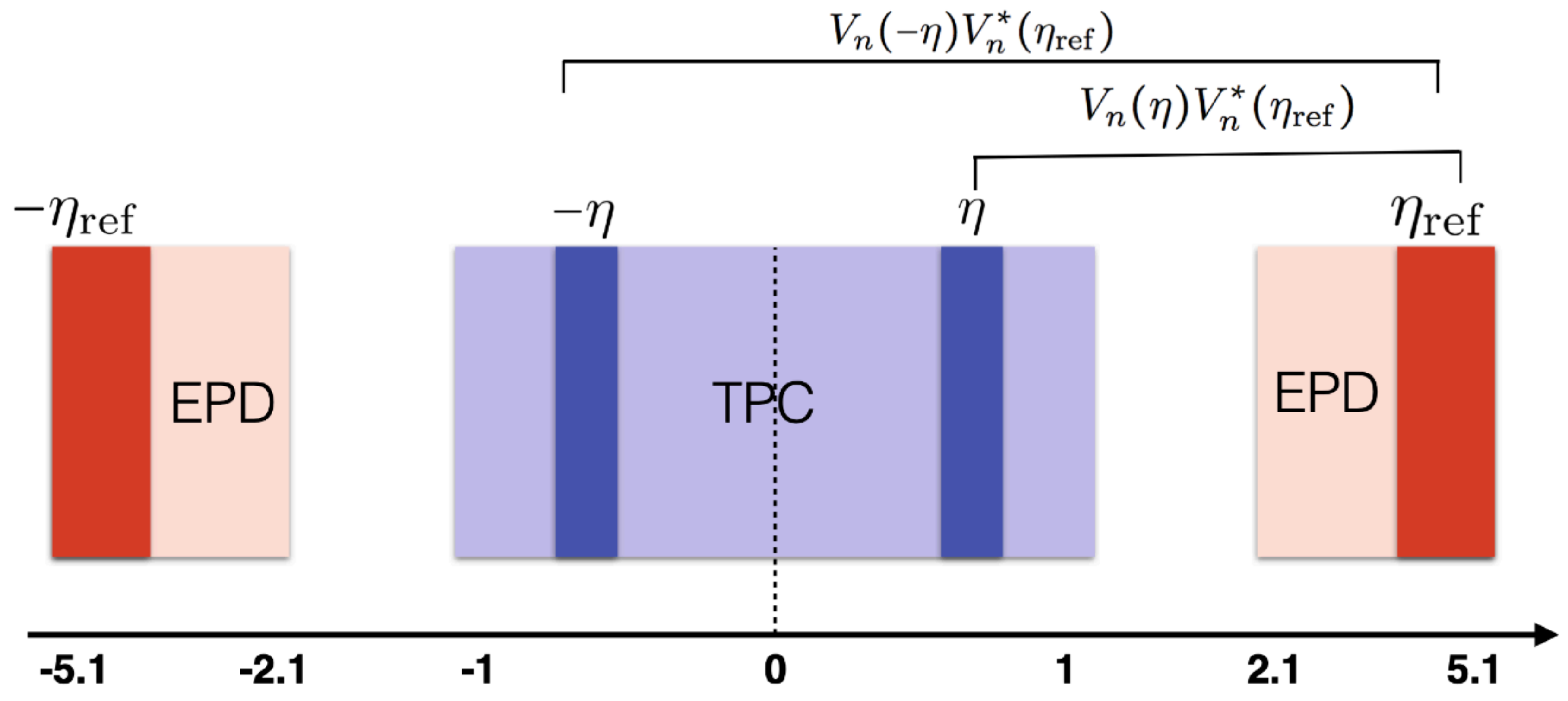

Longitudinal dynamics can provide the full space-time evolution of the fireball.

A large η gap is imposed to avoid short-range correlations.

STAR

Longitudinal flow correlations

For more information please see **Maowu Nie** poster:
https://indico.cern.ch/event/854124/contributions/4135474/

Energy dependence of v_2 decorrelation

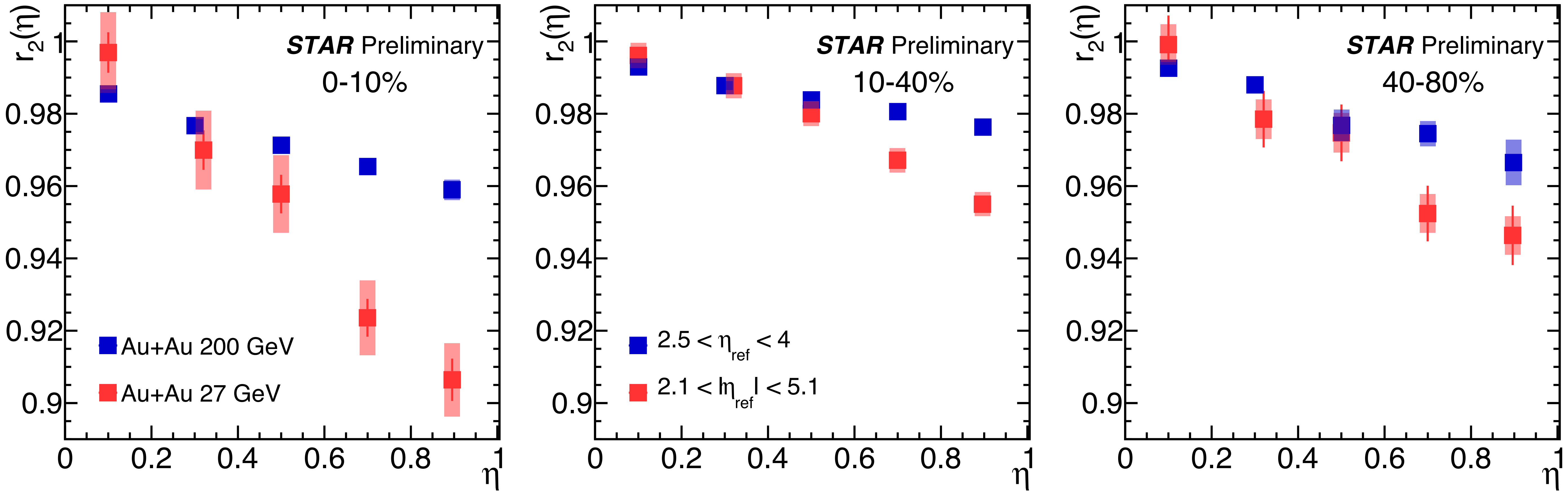

r_2 comparison between 27 GeV and 200 GeV

- Strongest v_2 decorrelation at 27 GeV is observed for all shown centralities.
- v_2 decorrelation at 27 GeV is ~2 times larger than at 200 GeV.

Energy dependence of v_3 decorrelation

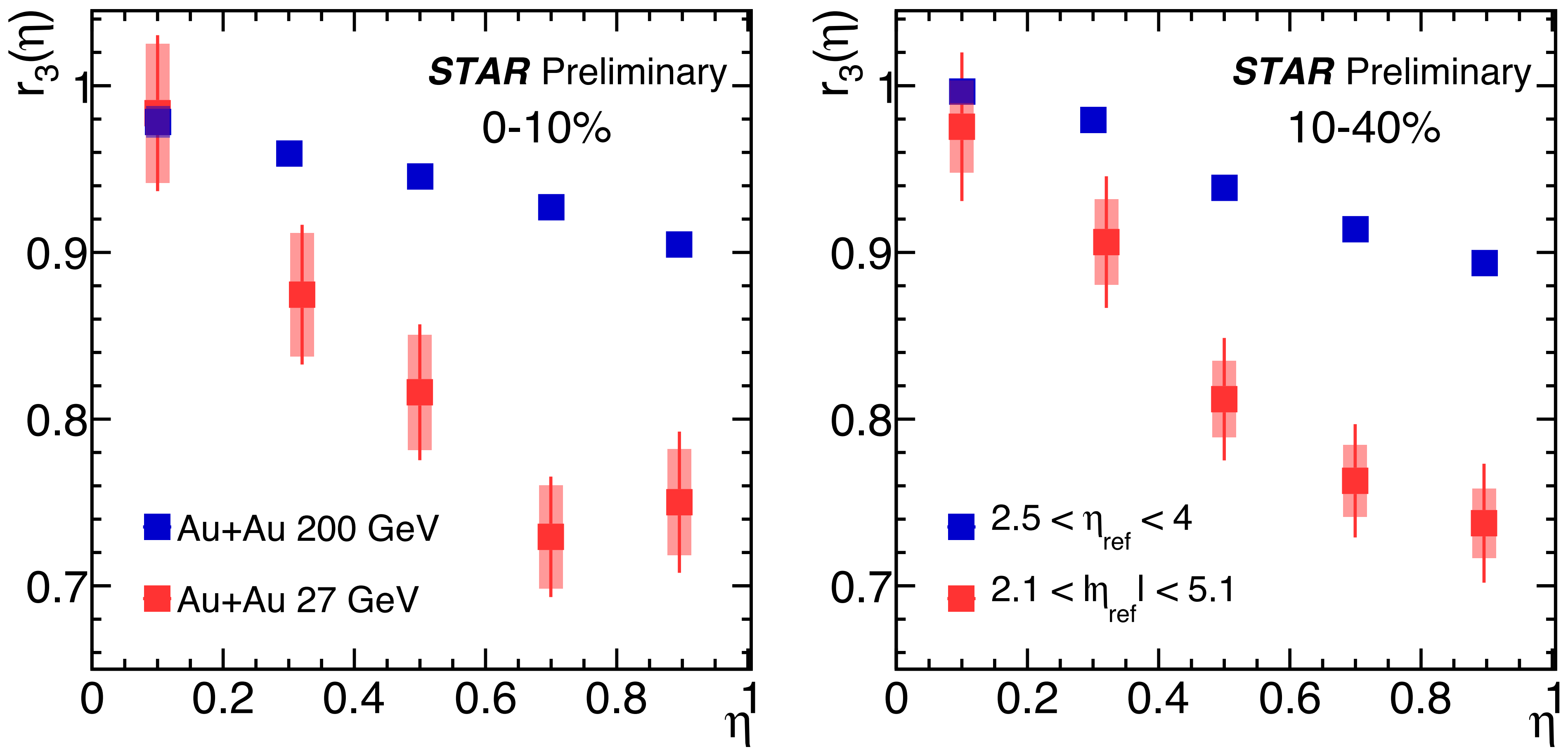

r_3 comparison between 27GeV and 200GeV

- Stronger v_3 decorrelation at 27 GeV is observed for the two centralities.

Longitudinal flow correlations

For more information please see **Maowu Nie** poster:
https://indico.cern.ch/event/854124/contributions/4135474/

v_2 decorrelation scaled by beam rapidity

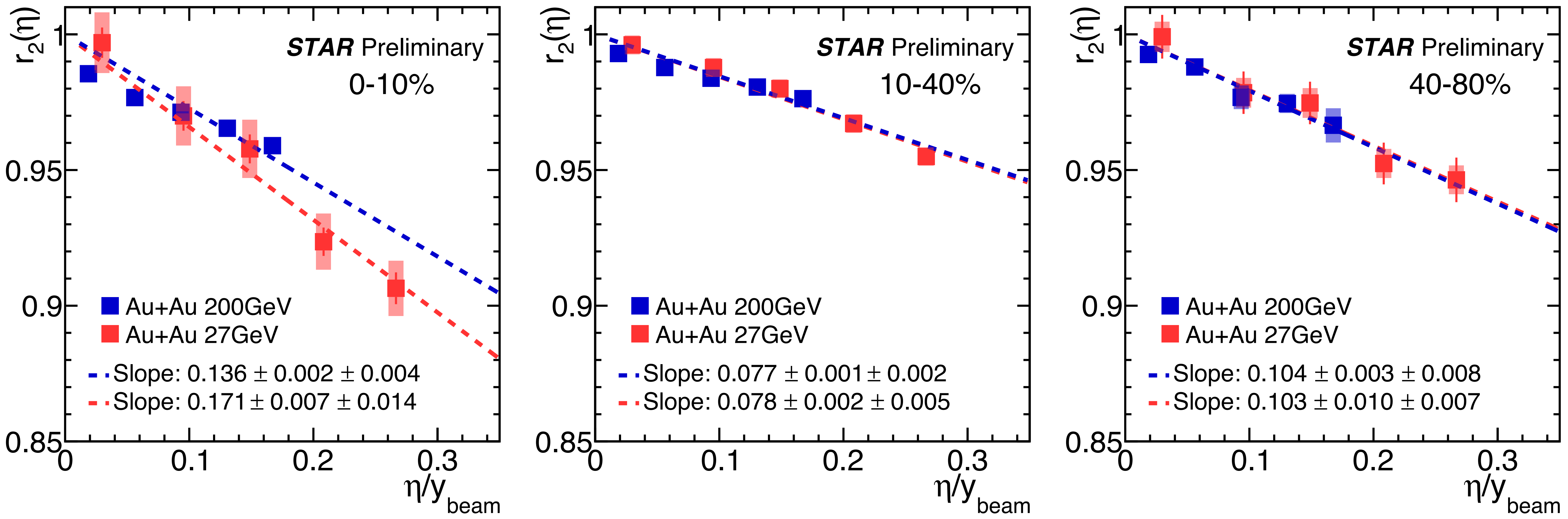

r_2 comparison between 27 GeV and 200 GeV with rapidity normalization

Even after y_{beam} normalization, r_2 shows:

- ◆ 0-10% weak energy dependence;
- ◆ 10-40% & 40-80% no energy dependence.

v_3 decorrelation scaled by beam rapidity

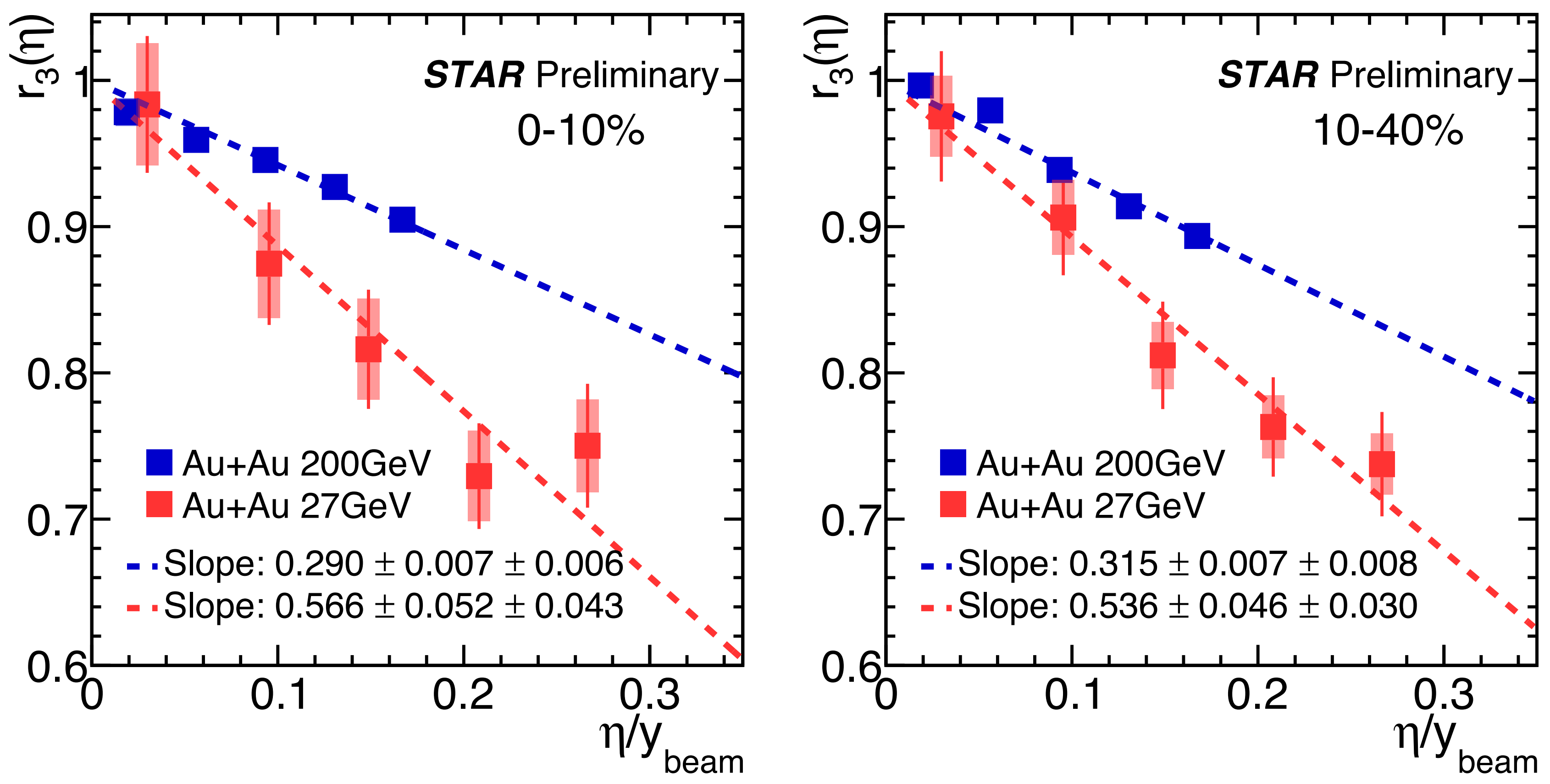

r_3 comparison between 27 GeV and 200 GeV with rapidity normalization

- ◆ Stronger v_3 decorrelation at 27 GeV after y_{beam} normalization…

High p_T flow harmonics

For more information please see **Niseem Magdy** poster:
https://indico.cern.ch/event/854124/contributions/4135478/

- The two-particle flow harmonics contains short- and long-range non-flow correlations:
  - Short-range non-flow effect gets reduced using |Δη| > 0.7 cut
  - Long-range non-flow effect gets reduced using:
    - Peripheral Subtraction
    - Global Momentum Conservation $v_n^{ab} = v_n^a v_n^b + \delta_{short} + \delta_{long}$

The STAR collaboration PLB 784 (2018) 26-32

$$v_{11} = v_{1a}v_{1b} - Cp_{Ta}p_{Tb}$$

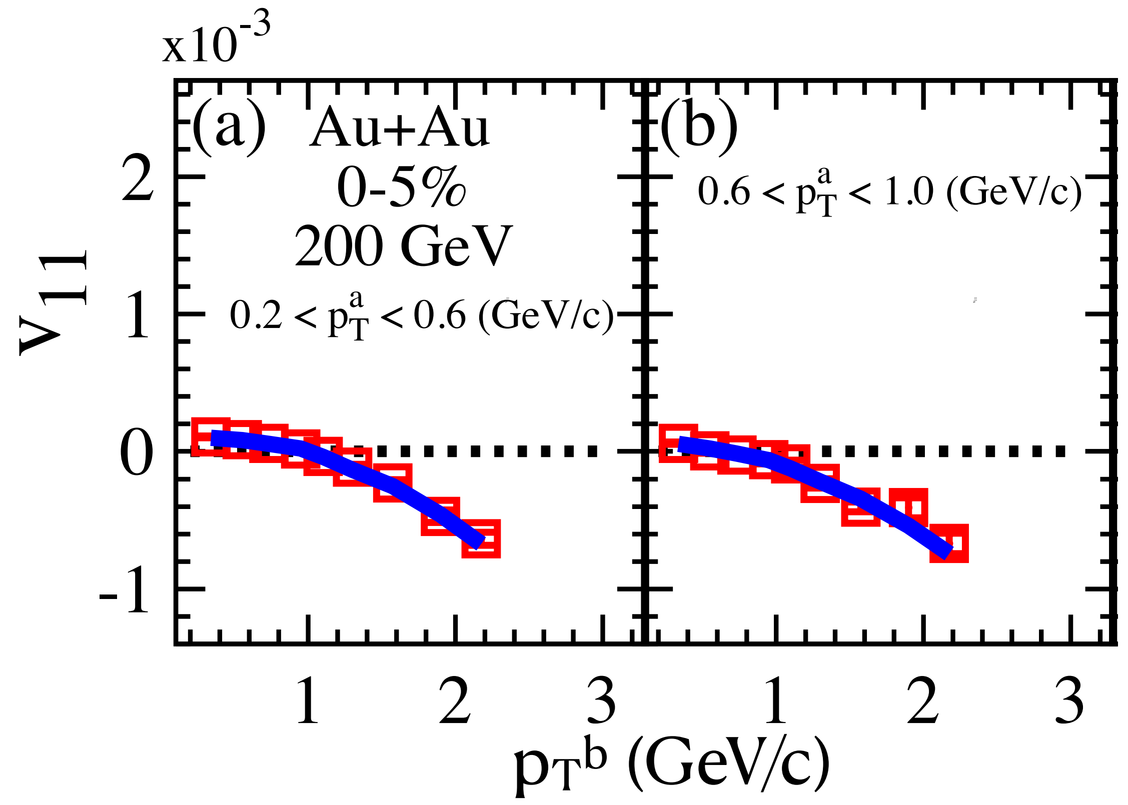

- Peripheral Subtraction

$$v_{nn}^{PS}(p_T) = v_{nn}^{cent\%}(p_T) - \chi^{cent\%}(p_T)\, v_{nn}^{90\%}(p_T)$$

$$\chi^{cent\%}(p_T) = v_{11}^{cent\%}(p_T)/v_{11}^{90\%}(p_T)$$

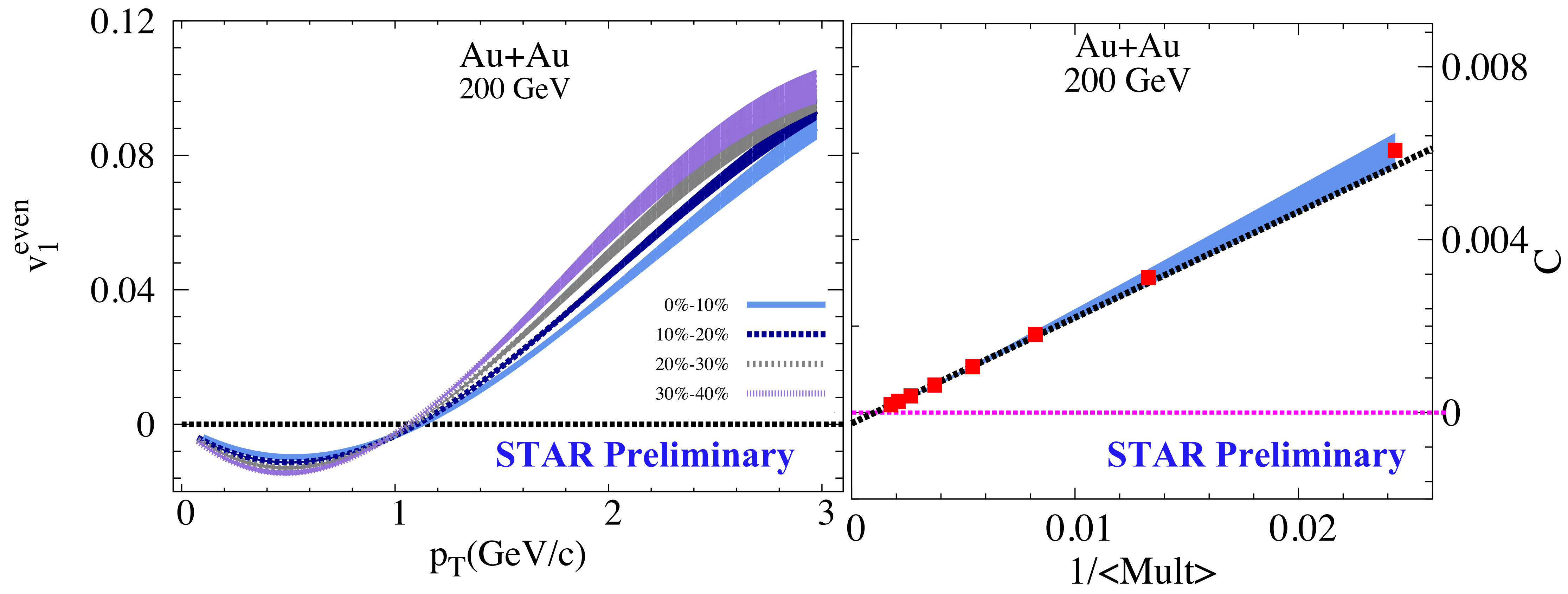

- Global Momentum Conservation

$$v_{nn} = v_{nn}^{flow} - C\,(\bar{v}_{n+1\,n+1} + \bar{v}_{n-1\,n-1})$$

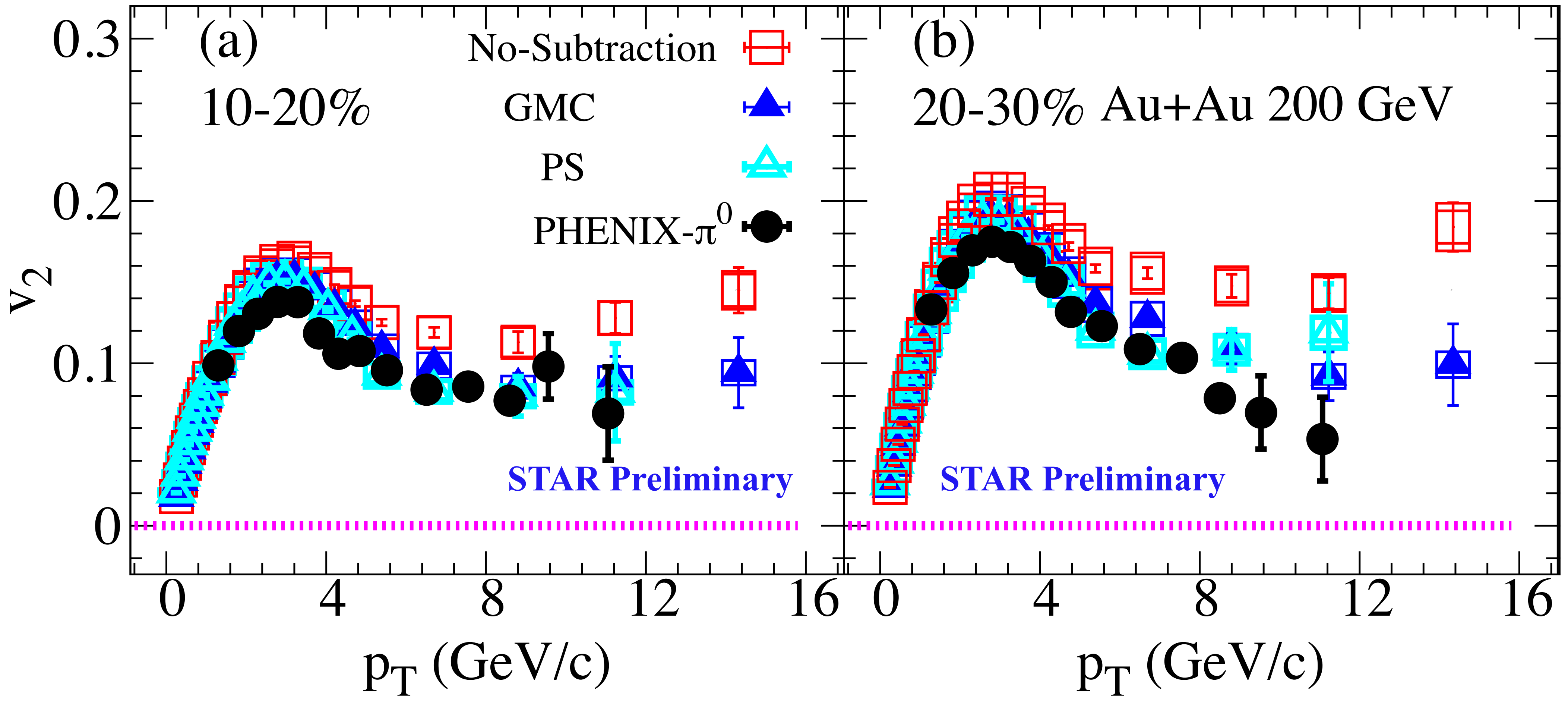

- Good agreement observed between;
  - GMC and the peripheral subtraction methods
  - STAR after the subtraction and PENIX π⁰ measurements

High p_T flow harmonics

For more information please see **Niseem Magdy** poster:
https://indico.cern.ch/event/854124/contributions/4135478/

v_2 (p_T) compared to similar LHC

The ALICE collaboration
JHEP 07 (2018) 103, 2018

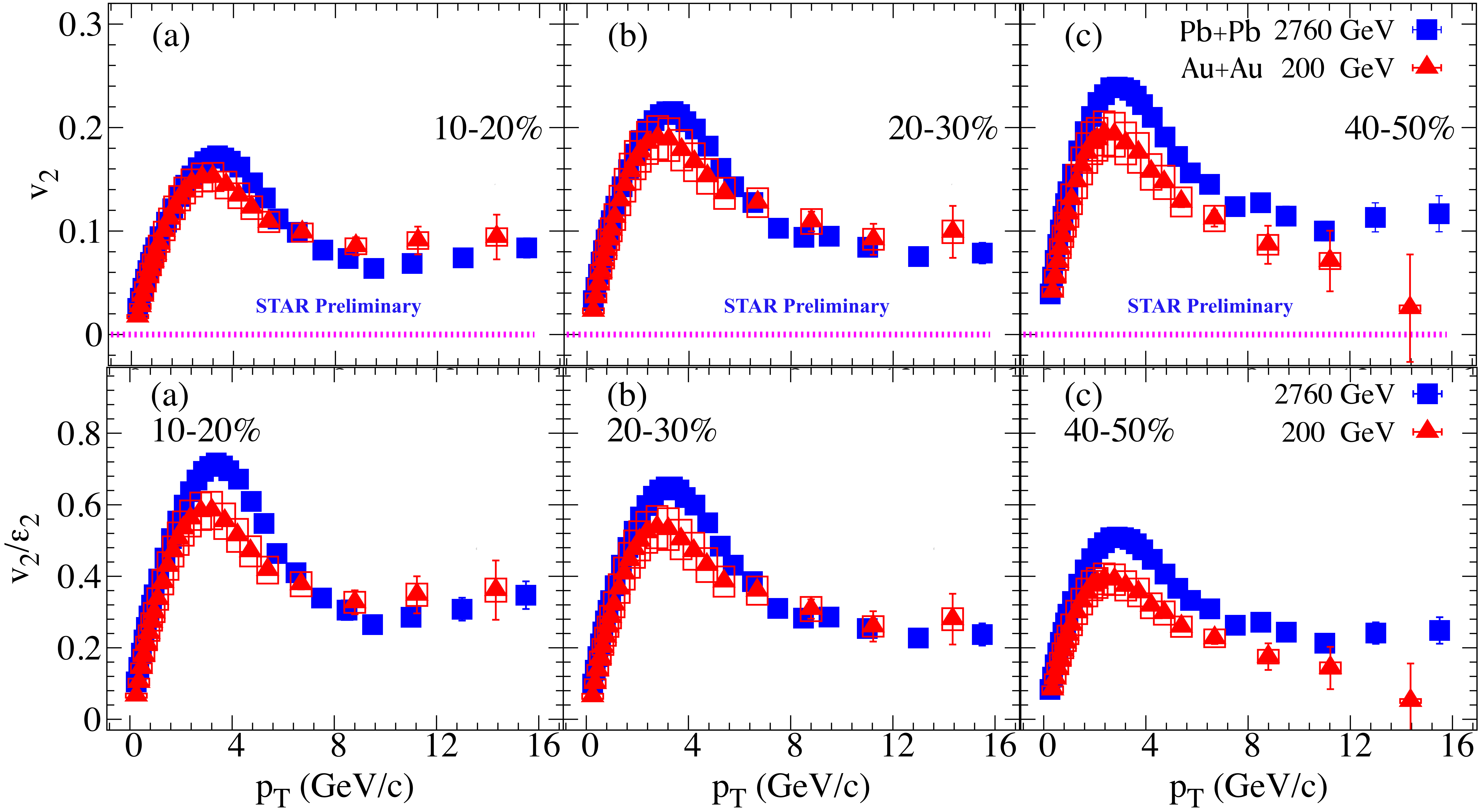

- ✦ v_2 (p_T) for high and low p_T show similar trend to the LHC data
- ✦ Measurements of high p_T v2 will add an additional constrain on energy dependance of $\hat{q}/T^3$

High p_T flow harmonics

For more information please see **Niseem Magdy** poster:
https://indico.cern.ch/event/854124/contributions/4135478/

The collision-system size dependence of v_n (p_T)

- v_2 (p_T) for high and low p_T show a collision-system size dependence
- v_3 (p_T) for high and low p_T are collision-system size independent
- v_n (p_T)/ε_n scales into one curve

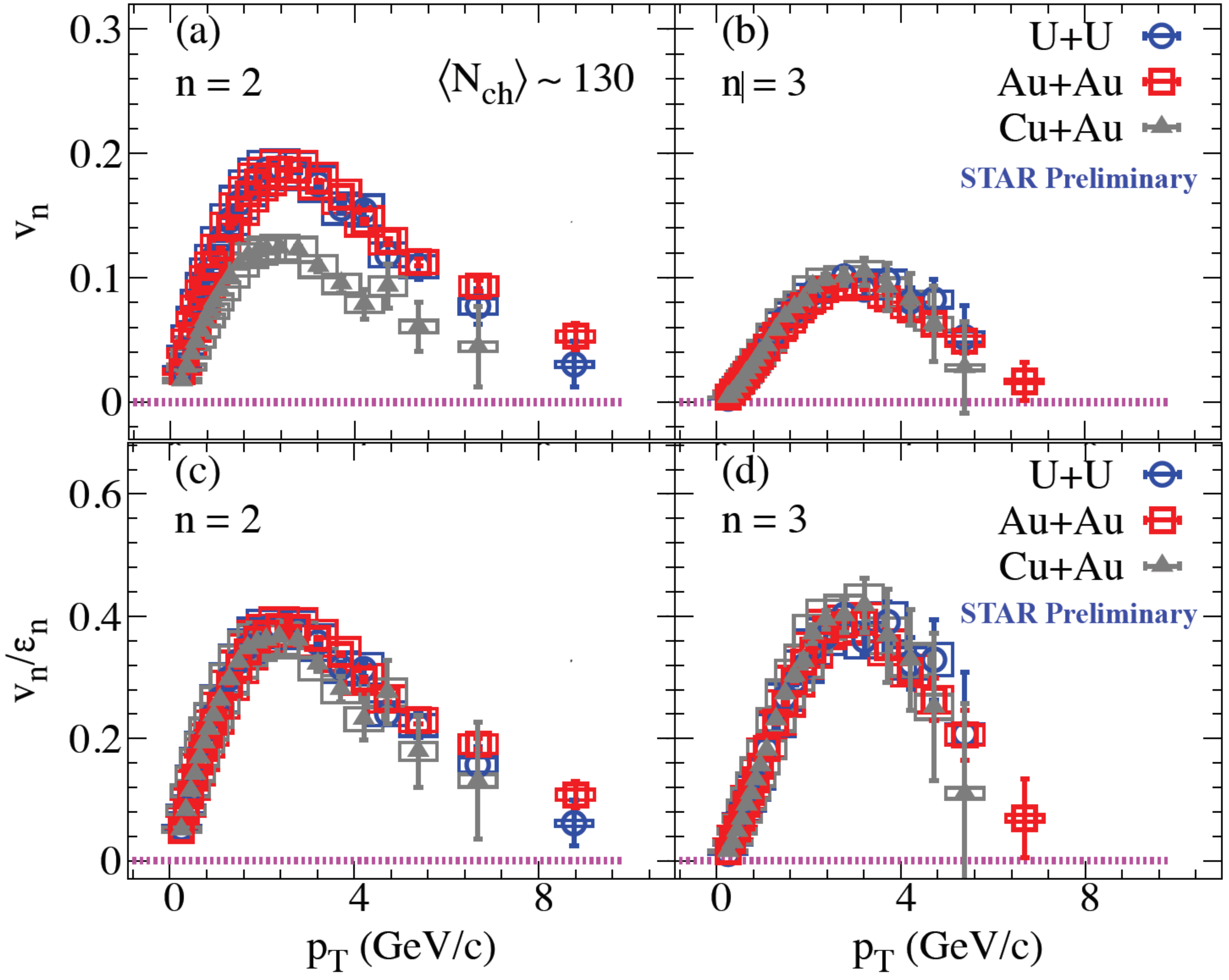

✦ **The $v_n(p_T)$ measurement will add additional constrain on the path length dependence of the energy loss**

STAR

Summary

- Identified hadrons flow harmonics:
  - Eccentricity does not differ relevantly between examined collision energies - differences caused by transitions in transport coefficients
  - Mass ordering present for v_2 and v_3 for $\sqrt{s_{NN}} = 39$ and 200 GeV
  - Similar trends of differences between triangular flow of particles and antiparticles as in elliptic flow

Summary

- Identified hadrons flow harmonics:
  - Eccentricity does not differ relevantly between examined collision energies - differences caused by transitions in transport coefficients
  - Mass ordering present for v_2 and v_3 for $\sqrt{s_{NN}} = 39$ and 200 GeV
  - Similar trends of differences between triangular flow of particles and antiparticles as in elliptic flow
- Longitudinal flow decorrelations:
  - Energy dependence of longitudinal flow decorrelation at RHIC provide new constraints on longitudinal dynamics of heavy-ion collisions
  - After beam rapidity normalization, r_2 shows no clear energy dependence, while r_3 still has clear energy dependence

Summary

- Identified hadrons flow harmonics:
  - Eccentricity does not differ relevantly between examined collision energies - differences caused by transitions in transport coefficients
  - Mass ordering present for v_2 and v_3 for $\sqrt{s_{NN}} = 39$ and 200 GeV
  - Similar trends of differences between triangular flow of particles and antiparticles as in elliptic flow
- Longitudinal flow decorrelations:
  - Energy dependence of longitudinal flow decorrelation at RHIC provide new constraints on longitudinal dynamics of heavy-ion collisions
  - After beam rapidity normalization, r_2 shows no clear energy dependence, while r_3 still has clear energy dependence
- High p_T flow harmonics
  - We observe a good agreement between GMC and the peripheral subtraction methods
  - v_2 at RHIC shows a similar p_T dependence to LHC data in a wide range of p_T.
  - Our high p_T measurements will add additional constrain on the path length dependence of the energy loss.

Summary

- Identified hadrons flow harmonics:
  - Eccentricity does not differ relevantly between examined collision energies - differences caused by transitions in transport coefficients
  - Mass ordering present for v_2 and v_3 for $\sqrt{s_{NN}} = 39$ and 200 GeV
  - Similar trends of differences between triangular flow of particles and antiparticles as in elliptic flow
- Longitudinal flow decorrelations:
  - Energy dependence of longitudinal flow decorrelation at RHIC provide new constraints on longitudinal dynamics of heavy-ion collisions
  - After beam rapidity normalization, r_2 shows no clear energy dependence, while r_3 still has clear energy dependence
- High p_T flow harmonics
  - We observe a good agreement between GMC and the peripheral subtraction methods
  - v_2 at RHIC shows a similar p_T dependence to LHC data in a wide range of p_T.
  - Our high p_T measurements will add additional constrain on the path length dependence of the energy loss.

Thank you for your attention

STAR